Ch 5
(265/1959)

UDC 669.275.24.3:621.762

# ACTA POLYTECHNICA SCANDINAVICA

**CHEMISTRY INCLUDING METALLURGY SERIES No. 5**

*SIMO MÄKIPIRTTI*

## On the sintering of W-Ni-Cu heavy metal

*Finnish Contribution No. 10*

HELSINKI 1959

## ACTA POLYTECHNICA SCANDINAVICA

*. . . a Scandinavian contribution to international engineering sciences*

Published under the auspices of the Scandinavian Council for Applied Research

in *Denmark* by the Danish Academy of Technical Sciences

in *Finland* by the Finnish Academy of Technical Sciences, the Swedish Academy of Engineering Sciences in Finland, and the State Institute for Technical Research

in *Norway* by the Norwegian Academy of Technical Science and the Royal Norwegian Council for Scientific and Industrial Research

in *Sweden* by the Royal Swedish Academy of Engineering Sciences, the Swedish Natural Science Research Council, and the Swedish Technical Research Council

*Acta Polytechnica Scandinavica consists of the following sub-series:*

*Chemistry including Metallurgy Series, Ch*
*Civil Engineering and Building Construction Series, Ci*
*Electrical Engineering Series, El*
*Mathematics and Computing Machinery Series, Ma*
*Mechanical Engineering Series, Me*
*Physics including Nucleonics Series, Ph*

For subscription to the complete series or to one or more of the sub-series and for purchase of single copies, please write to

**ACTA POLYTECHNICA SCANDINAVICA PUBLISHING OFFICE**

Box 5073
Stockholm 5 Phone 61 47 53

**This issue is published by**
**THE FINNISH ACADEMY OF TECHNICAL SCIENCES**
**Helsinki, Finland**

UDC 669.275.24.3:621.762

# ON THE SINTERING OF W-Ni-Cu HEAVY METAL

by

*SIMO MÄKIPIRTTI*

ACTA POLYTECHNICA SCANDINAVICA
Mechanical Engineering Series ME 7
(AP 265, 1959)

VTT Rotaprintpaino 1959

CONTENTS

## PREFACE

This investigation constitutes part of a more extensive basic research entity which has as aim the determination of the behaviour of solids at high temperatures. The practical work and the measurements involved in the study were carried out during the years 1955 – 1959, mainly in the Laboratory of metallurgy of the Institute of Technology (Helsinki).

In this connection, I wish to express my gratitude towards the following members of the staff at Surahammars Bruks AB., Sweden: Mr. B. Skoog, M.Sc., Mr. S. Sandell, M.Sc., Mr. C. Ericsson, M.Sc. and Mr. R. Merl, M.Sc., who have obligingly aided me in this work. In the work of development and application of the necessary physical measuring methods I have received valuable help from Mr. B. Regnell, M.Sc., and Mr. I. Huhtinen, M.Sc., among others, and my sincere thanks are extended to them. I am similarly indebted to Mr. O. Tuori, M.Sc., who has given his kind assistance in the analytic work concerned with the investigation material.

Furthermore, I wish to express my thanks to Professor E. Laurila, Ph.D., for numerous valuable suggestions, and to Professor M.H. Tikkanen, D.Sc., for all the generous help he gave me during the time that I was pursuing this work under his supervision.

My gratitude is also due to the representatives of the Finnish Cultural Foundation (Suomen Kulttuurirahasto) and of the Finnish Scientific Research Council (Valtion Luonnontieteellinen Toimikunta), as well as to the Principal of the Institute of Technology (Helsinki) for the grants which made this work possible.

Finally, I wish to thank Mr. U. Attila, M.Sc., for his translation of the manuscript into English.

December 1959

Simo Mäkipirtti

# I REVIEW OF THE THEORY OF SINTERING

Sintering is a process in which metal or mineral powders are transformed into coherent solids at temperatures which are below the melting points of the components represented in the largest quantities in the system.

The most essential of the variables which control the process of sintering are temperature and time. Other factors of influence are the size, the shape and the surface condition of the powder particles, the conditions of compression, the sintering atmosphere, etc.

In recent years, the mechanism of sintering has been subject to considerable research work, particularly in the aspects which relate to the transport of material in the system.

## 1. THE FORMATION AND GROWTH OF CONTACT POINTS AND SURFACES

The first stage of sintering can be considered to consist of the formation of point bonds and bond areas between the powder grains. No satisfactory explanation has yet been found for the formation of the bonds, and most of the theories encounter surface and grain boundary problems which are as yet unsolved.

According to the theories of Schwarzkopf [1] and of Kingston and Hüttig [2], compression of a powder at room temperature (recrystallization and hot compression theory) induces nucleus formation along the points of contact between grains. According to Smekal [3], the low stresses occurring on packing and mixing the powder are already sufficient to produce bonds by way of surface fusion. Shaler [4] assumes that the bonds between the powder grains come into existence as the result of cold welding caused by the attractive forces between their surfaces. These

theories have the common feature that the initial bonds are assumed to exist in the powder packing even before sintering.

The growth of the point bonds and bond surfaces can be considered to be the second stage of sintering, and it is during this that the actual transport of material takes place. A great number of investigations have recently been carried out in order to elucidate the growth mechanism with the aid of ideal models (pair of spheres, sphere/plane, wire/plane, etc.) which by reason of their simple geometry enable a theoretical study of the phenomena to be made. It can be said, on the basis of the theories, that two fundamental mechanisms, diffusion flow and macroscopic flow, appear possible.

Diffusion sintering models which have been presented and criticized include those by Kuczynski [5], Cabrera [6], Schwed [7], Kingery and Berg [8], Herring [9] and Coble [10]. The material transport in the models is studied, as opposed to the vacancy flow. The neck of the non-spherical segment at the point of contact of two spheres (or some other combination) or the dislocations serve as vacancy sources. The gradient of the chemical potential produced by the change of surface curvature sets the vacancies into motion. The excessive vacancy concentration, as compared with the equilibrium value, under the surface of the neck between the spheres, has been calculated in the models on the basis of Kelvin's equation. In the case where the vacancies flow from the dislocations to the grain boundaries, the potential gradient in the direction of diffusion has not yet been quantitatively solved. In the models, the vacancy creation and annihilation have been assumed to be very rapid, so that the diffusion determines the rate. By equating the diffusion and vacancy flow rates, one obtains the sintering equation. The models presented by various investigators primarily differ in their choice of diffusion path. Since no exact analytical expression has been found for the diffusion flow, the sintering equations obtained by various approximations mainly differ as regards their constant factors.

According to the different models, the sintering equation has the general shape:

$$X = (k_0 t)^n, \tag{1.1}$$

where X stands for the variable quantity under consideration (e.g. the ratio of the radii of contact neck and sphere [5 ··· 10], the ratio of the compact volume or diameter to the initial value [8, 10], the ratio of the conductivities of the compact and of the dense substance [5]), t is the time, n a time exponent depending, among other things, upon the type of diffusion, and $k_0$ is a rate coefficient dependent upon temperature, involving in addition to the diffusion constant, general material and natural constants, numerical factors depending upon the geometry of the model, etc.

If one compares the diffusion constants derived from direct measurement and from sintering models, they are found to be of the same order of magnitude [5, 8]. The differences, in comparison with the absolute values, are due to the different approximations employed. The activation energies, as compared to the diffusion measurements, are equal in magnitude. The influence of grain size upon the sintering rate is the same for the different bulk diffusion models ($R^{-3}$, where R is the grain radius) [5, 8, 9].

An equation of the form 1.I too is obtained for the surface diffusion and evaporation-condensation mechanisms [5 ··· 10]. These mechanisms do not cause any densification of the powder compact, but their influence may be indirectly noticeable, causing a reduction of the potential gradient of bulk diffusion by its competitive effect.

If sintering were regulated by a diffusion mechanism, one might assume that the same result would be obtained during a certain adequate length of time, independent of temperature. Since this is not always the case, it has been thought that a macroscopic viscous or plastic flow is entirely or partially responsible for the transport of material.

Viscous, as well as plastic flow, involves shearing of the material. The flow is viscous if the rate of shearing is directly proportional to the shearing stress (Newtonian flow: $dS/dt = \sigma/\eta$, where S is the strain, $\sigma$ is the shearing stress, and $\eta$ the coefficient of viscosity); it is plastic if shearing occurs only above a given critical stress (Bingham's law: $dS/dt = (\sigma - \sigma_y)/\eta$, where $\sigma_y$ is the yield stress).

Frenkel [11] has shown that crystallites can grow together at sintering temperature by reason of Newtonian flow (the sintering equation has the form 1.I). The law has been found to be valid [5, 8] on the sintering of glass spheres. Shaler et al. [4] state that the sintering of copper spheres, at a late stage at least, proceeds by means of viscous flow. The results obtained have also been found to be compatible with the theory of diffusion [4, 5].

In addition to the models of Frenkel, and those of Shaler and Wulff, two other models have been constructed in order to elucidate the process of sintering, namely, those of Shuttleworth and Mackenzie [12] and of Clark and White [13]. In these models, the rate equations have been presented for both kinds of flow. Reconciliation of experimental results and theory has been partly achieved by means of a correction factor. Application of the experimental results to both models has demonstrated their mutual agreement over an extensive sintering range [13].

Since both the diffusion flow model and the macroscopic flow model possess their advantages in the treatment of sintering problems, it is a difficult matter to make any conjecture on the basis of the investigations mentioned as to which of these conceptions is the correct one.

## 2. THE DISAPPEARANCE OF CLOSED PORES

The last stage of sintering starts when the pores have become closed and isolated from each other. In this stage, only bulk diffusion or macroscopic flow may be significant, because the evaporation-condensation mechanism or the surface diffusion mechanism can change only the shape of the pores, and not their size.

The validity of the bulk diffusion mechanism in the last stage of sintering was at first disputed on the grounds [12] that after closure of the pores the vacancy diffusion on the surface of the packing is too slow in its relation to the observed sintering rates. Subsequently, however, the presence of a vacancy destruction mechanism in the metal itself has been shown (Smigelskas and Kirkendall [14], Sylva and Mehl [15]). The vacancies are resolved at certain points in the lattice, e.g., mosaic and grain boundaries, dislocations, and so on. Nabarro [16] has also presented a vacancy destruction mechanism and shown its compatibility with Kuczynski's model.

The changes in the pore volume and the total porosity have been studied quantitatively by Rhines in his remarkable work [17]. In his investigation, the bulk diffusion is assumed to determine the sintering rate (the reasoning is that formation of a dislocation requires more energy than that of a lattice vacancy; furthermore, macroscopic flow is unable to account for the observation that the size of individual pores may increase with decreasing total porosity). Alexander and Balluffi [18] note that the bulk diffusion mechanism governs the sintering during the disappearance of the isolated pores, as well as in the other stages of sintering. The importance of the grain boundaries in the final stages of sintering has also been considered qualitatively by Balluffi and Seigle [19], Burke [20], Kuczynski [5] and others, while quantitative studies of this aspect were made by Kingery and Berg [8], who arrived at results similar to those obtained by the above-mentioned investigators.

## 3. TECHNICAL METAL POWDERS AND POWDER MIXTURES

Technical metal powders, with their wide range of grain size distribution, present extreme difficulties as objects of investigation owing to the complicated geometry of the systems concerned.

An outstanding theoretical work is Bockstiegel's [21] investigation, in which Kuczynski's model is considered in its application to powder grains of irregular shape.

The sintering equation derived from the considerations has the form

$$X(t) = X(\tau)[t/\tau]^n \qquad 2.I$$

where $X(\tau)$ is the change occurring during the time interval $\tau$ ; X stands for the contact surface area of the grains, the tensile strength, the change in diameter of the test specimen, Okamura's [22] ratio, or other similar variables, while the time exponent n is composed of two factors, one of them depending upon the shape of the grains, and the other upon the type of material transport (i.e., the geometric and kinetic factor, respectively).

One-component systems (Fe, Ni, Ag, Cu) of technical metal powders have been investigated, among others, by Okamura [22], Masuda, Kikuta [23] and Takasaki [24]. Sintering of the powders was found to be a rate process, and to have the form, isothermally,

$$(V_o - V_s)/(V_o - V_m) = At^n, \qquad 3.I$$

where $V_o$, $V_s$ and $V_m$ are the specific volumes of the compact before and during sintering and after sintering to a dense state, respectively; n is a time exponent ($<1$) depending, among other things, upon the material quality, and A is a constant dependent upon temperature. The observed activation energy values were somewhat different from the corresponding values of self-diffusion. The water content of the protective gas appeared amongst other things to have an effect upon the height of the activation energy [24].

Cizeron and Lacombe [25] have dilatometrically investigated the sintering of carbonyl iron at temperatures below 900°C. The linear shrinkage of the test specimen obeyed a law of the form

$$L = 1 + K[t \exp(-Q/RT)]^n, \quad n>0, \text{ and} \qquad 4.I$$

$$L = L_\infty - K'[t \exp(-Q/RT)]^{n'}, \quad n'<0,$$

where $L_\infty$ is the asymptotic shrinkage percentage, and K, K', n and n' are constants. The time exponent was not constant, but changed with time and temperature. It was noted in the investigation that the sintering is governed at low temperatures by the bulk diffusion and at high temperatures, upon closure of the pores, by the grain boundary diffusion mechanism. For the activation energies, values approximating to their theoretical magnitude are obtained.

The investigation of powders of metals with allotropic transformations (e.g. Fe: Duwez and Martens [26], Cizeron and Lacombe [25]; Zr: Hausner [27]; Th: Meechan [28], etc.) yielded a strong argument in favour of the diffusion theory of sintering. On either side of the transformation point, a result is obtained that can be derived from the different diffusion properties of the respective structures.

A powder system made up of two or three components is already extremely complicated. There are very few investigations in this sphere, because as yet the one-component system and the intermetallic diffusion have not been completely mastered.

In the two-component powder system, the sintering is related to the mutual solubility of the components.

If the solid solubility of the components in each other is very low, interdiffusion will not affect the result. The powder is then sintered in the manner of a one-component system, i.e., either component is sintered in its own temperature range and in accordance with its material characteristics (e.g. Ag-Fe: Raub [29], Cr-$Al_2O_3$-cermet: Onitsch-Modl [30]).

If the components have a limited solubility, and intermetallic compounds occur, the sintering will be highly complicated. During the sintering, all the intermetallic phases of the phase diagram are usually involved. If the temperature is insufficiently high, the sintering may stop at a pseudo-equilibrium, the stable compound being in equilibrium with the remaining part of the pure component. The agent which slows down or stops the process may be a super-lattice, or the phase that is most stable under the conditions. An increase in the temperature above the stable range of the obstacle will cause resumption of sintering and interdiffusion (Cu-Sn, Cu-Au: Duwez and Jordan [31]). Interdiffusion may also take place without simultaneous sintering (Cu-Zn: material is transported in the gaseous phase [31]).

When the components are mutually completely soluble, interdiffusion and sintering occur simultaneously. The majority of the investigations which relate to this sphere are concentrated on interdiffusion: the relation of interdiffusion and sintering occurs only qualitatively, or not at all. According to these investigations, the mutual diffusion of the components in the powder packing can be noted as obeying the well-known laws of diffusion (Cu-Ni: Duwez [31], Weinbaum [32]). The interdiffusion of copper/nickel powder mixture has been extensively investigated by means of magnetic analysis (Torkar [33], Köster [34]). For the activation energy of diffusion, the approximate theoretical value has been found [34]. It is of particular note in these investigations that the mixed crystal yield which corresponds to the nominal composition of the mixture is a function of the density of the powder packing [33]. This shows that there is a relationship between interdiffusion and sintering, binding at least one of these processes. A relationship of the same kind can also be deduced from the conductivity measurements with Fe-Si systems carried out by Glaser [35]. Butler and Hoar [36] note,

in contradistinction to the above that as a result of dilatation measurements (Cu-Ni), interdiffusion and sintering admittedly occur simultaneously but that they are not mutually related.

In multi-component systems, the influence of interdiffusion upon sintering, at least transiently in the formation of highly active states (Hedvall and Kirkendall effects), in an undisputable fact [37, 38].

## 4. THE OBJECT OF THE PRESENT INVESTIGATION

In the present work an attempt will be made to determine, on the basis of present theory, the behaviour of the tungsten-nickel-copper powder system during sintering at high temperatures. The composition of the mixture has been chosen from the heavy metal alloy range, which has the greatest practical significance. The use of heavy alloys has been steadily expanding, and new fields of application are being continuously opened for such mixtures by the rapid technical development of today. Heavy alloys are being used in instrument manufacture (precision watch mechanisms, speed and acceleration indicators, gyro mechanisms, torpedo components, bomb sights, flow meters, etc.), in aircraft manufacture (balancing of rotors, propellers, stabilizers etc., flywheels in the Maxaret system etc.), for radioactive shielding, and so on.

A study of relevant publications, together with general experience, justifies the statement that rather little has been done so far to investigate the sintering phenomena concerned. This has to be attributed to the comparatively difficult experimental conditions, and to the lack of a consistent analytical description which is valid for the entire range of sintering, both in the one-component and the multi-component systems.

## II EXPERIMENTAL PROCEDURE

### 1. RAW MATERIALS AND PREPARATION OF THE TEST SPECIMENS

For the sintering experiments, use was made of electrolytic copper powder, carbonyl nickel powder and tungsten powder reduced from tungstic acid. The grain size distribution of the powders was analyzed by means of the Sharples apparatus [1], the results being shown in Fig. 1. In addition to these powders, ready-alloyed Monel powder was used. This powder had a grain size of about -53 $\mu$, and an analysis of 67.0 % Ni, 30.0 % Cu, 1.5 % Fe and 1.0 % Mn[2].

The actual mixture to be investigated was prepared by mixing together 90 % tungsten powder and 10 % of a powder mixture containing copper and nickel in the proportion of 2 to 1. Furthermore, an investigation was made of powder mixtures of the composition 90 % tungsten and 10 % Monel powder and 90 % tungsten and 10 % nickel powder. The mixtures mentioned will be referred to by the notations 90W.10(2Ni.Cu), 90W.10Monel, and 90W.10Ni, respectively. Camphor was added to the carefully mixed powders in order to facilitate their compression.

Test specimens were prepared in the form of cylinders, of 18.5 mm diameter and 3 to 4 mm in height, dependent upon the compression pressure. The material in each cylinder amounted to about 10 g. The test specimens were subjected to compression in a material testing machine (Amsler & Co) of 50 tons capacity. All specimens were compressed in the same manner. The variation of compression pressure was about $\pm$ 0.01 tons per cm$^2$.

---

1) The author is indebted to the company Oy Airam Ab for the use of their facilities.

2) In this work, all quantities of material are given as percentages by weight, unless otherwise stated.

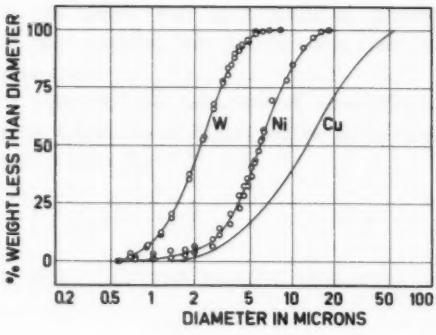


Fig. 1. Grain size distribution of the W, Ni and Cu powders.

For investigation of the properties of the sintered test specimens, there were prepared standard tension bars of 90 mm length, and bars of dimensions 7x7x59 mm. The bars, which contained about 25 g of material, were compressed at about 4 tons per $cm^2$.

## 2. MEASUREMENT OF THE DILATATION OF THE TEST SPECIMEN AT HIGH TEMPERATURES

### 2.1 Design of the measuring equipment

The dilatation measurements were carried out by the photographic method of determination of the linear dimensional changes of the test cylinder.

The measuring equipment consisted of a sintering furnace with its power supply and temperature control equipment, a protective gas purifier, a temperature measuring device and the photographic apparatus. The furnace arrangement is shown in the drawing in Fig. 2.

The power supply of the furnace (60 amperes, 40 volts) and its temperature control were effected in accordance with the circuit diagram in Fig. 3. The accuracy of temperature control was $\pm 1^{\circ}C$.

The temperature of the specimen was measured in accordance with Figs. 2 and 3, employing a precision potentiometer (Rubicon Co.). A platinum vs. platinum + 10 % rhodium thermocouple (J.M.C.) was used for the measurements; this thermocouple was calibrated from time to time by comparison with the standard thermocouple of the laboratory.

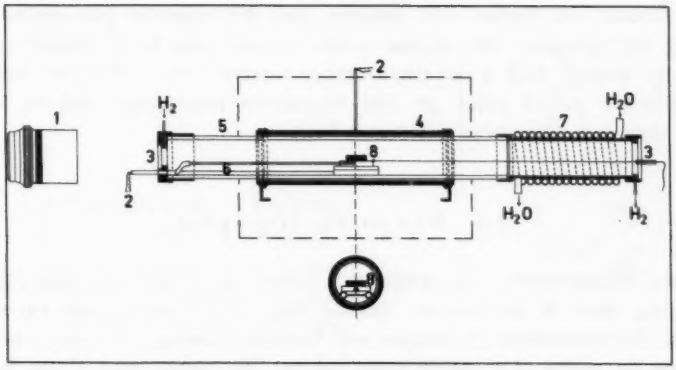


Fig. 2 Schematic diagram of the furnace arrangements: 1. Optics, 2. Thermocouples, 3. Windows, 4. Silicium carbide resistance tube, 5. Furnace tube, 6. Stop rod, 7. Cooler, 8. Boat and specimen.

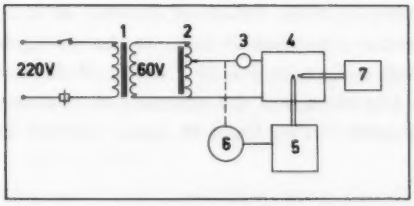


Fig. 3 Furnace control system: 1. Transformer, 2. Variac, 3. Ammeter, 4. Furnace, 5. Honeywell temperature controller, 6. Servomotor, 7. Potentiometer.

The test specimens were photographed on 24 x 36 mm film frames, using an Exacta Varex camera. The objective was a Tele-Megor with a focal distance of 400 mm, used with an extension tube of appropriate length to produce an image on the film equal in size to the test specimen.

The furnace was flushed with nitrogen, and the protective gas applied during sintering was hydrogen. The oxygen present in the gases as an impurity was removed by burning with a hot silica-copper catalyst [39]. The gases were then dried with the aid of silica gel and magnesium perchlorate, and led into the furnace through a flow meter (Fischer & Porter).

### 2.2 Measuring procedure

For the measurement, the specimen, placed in a boat, was first placed in the cooling zone of the furnace, and the plug of the furnace tube was screwed in. After the completion of nitrogen and hydrogen flushing, the boat was rapidly pushed by means of a molybdenum rod into the hottest zone of the furnace. The specimen was photographed at certain intervals in correspondence with the rate of sintering. When the treatment had been completed, the boat was rapidly drawn into the cooling zone, and finally out of the furnace.

The films, developed at high contrast, were evaluated directly as negatives, measuring them in the Leitz measuring microscope. The accuracy of measurement was about $\pm$ 0.03 %.

For calibration of the measuring equipment, the thermal expansion of Armco iron (99.94 % Fe) was measured [40]. The measurement yielded, for $\alpha$-iron in the interval 20° - 800° C the linear thermal expansion coefficient $\beta_\alpha$ = 15.8 x $10^{-6}$ 1/°C and for $\gamma$-iron in the interval 925° - 1300°C $\beta_\gamma$ = 24.6 x $10^{-6}$ 1/°C. In the temperature interval of 800° - 920°C, a considerable anomalous region due to magnetostriction and $\alpha/\gamma$-transformation was observed. If one calculates from the lattice constant values of Basinski et al. [41], one finds for the coefficient of thermal expansion of iron, in the $\alpha$-region $\beta_\alpha$ = 15.3 x $10^{-6}$ 1/°C and in the $\gamma$-region $\beta_\gamma$ = 23.8 x $10^{-6}$ 1/°C. If there is taken into account the difference due to impurities and the accuracy of measurement, the result obtained in the present work is thus found to agree with the above-mentioned investigation.

## 3. OTHER MEASURING METHODS

### 3.1 Measurement of electrical conductivity

Electrical conductivity was measured by means of leading a known current (10 A) through the ends of the test bar, and measuring the potential difference between contact tips in the middle of the bar with a vacuum tube voltmeter. This arrangement had the advantage of eliminating the effect of contact resistances upon the results of measurement.

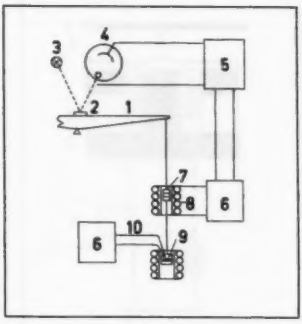


Fig. 4 Automatic balance: 1. Weighing-beam, 2. Mirror, 3. Lamp, 4. Photoelectric cell, 5. D.C. amplifier, 6. Potentiometer recorder, 7. Permanent magnet, 8. Coil, 9. Specimen, 10. Thermocouple.

The conductivity of the cylindrical samples was measured by a comparison method, using the Sigma-test instrument.

### 3.2 Measurement of magnetic properties

The device employed to determine the Curie temperature is schematically shown in Fig. 4. The force required to balance the weighing-beam, which is a function of the magnetization of the specimen, was recorded with the aid of a recording potentiometer. Since the Curie points were as a rule below room temperature, the specimen was enclosed in an aluminium cylinder lined with cork and submerged in liquid oxygen. When the specimen had cooled down, it was inserted in the magnetizing coil, and connected to the weighing-beam. The temperature of the specimen was measured by means of a copper-constantan thermocouple in contact with its side. The change of temperature was recorded by means of a potentiometer recorder.

Hysteresis measurements of the specimens were carried out only as relative measurements, using a Hall generator apparatus [40].

### 3.3 Measurement of damping

The device for the measurement of damping is schematically shown in Fig. 5. The current supplied by an oscillator produces a force in the coil moving in the field of a permanent magnet, and this force generates vibrations of the bar. The frequency is altered until the resonance frequency $f_0$ of the transversal oscillation is found, at which point the amplitude of oscillation is maximum. Let the corresponding voltage be U. If the frequency is increased and decreased to an extent

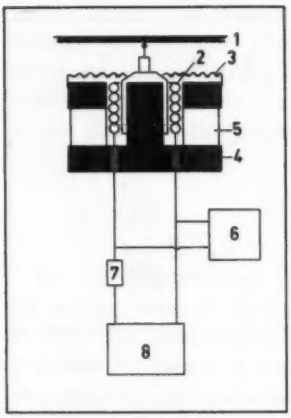


Fig. 5 Damping measuring equipment: 1. Test bar, 2. Coil, 3. Memprane, 4. Soft-iron core, 5. Permanent magnet.

sufficient to bring the voltage down to $\sqrt{2}$ U/2, and then the corresponding frequencies $f_1$ and $f_2$ are read, the quality factor is obtained, by definition, from the formula $Q = f_o/(f_1 - f_2)$. As a measure of damping, its inverse value $Q^{-1}$, or the width at half of the maximum intensity itself, is usually employed.

### 3.4 X-ray methods

In the x-ray investigation of the samples, an automatically recording goniometer (Norelco) and a 114,59 mm camera were employed. The radiation was Co and Cu radiation, filtered through Fe or Ni foils if needed.

In the determination of the lattice constants, the endeavour was that of obtaining lines at angles of reflexion in excess of 80 degrees. In the extrapolation of the lattice constants, the correction functions [42] $a' = F(1/2(\vartheta^{-1}\cos^2\vartheta + \sin^{-1}\vartheta\cos^2\vartheta))$ and $a' = F(\cos\vartheta)$ were used.

The samples for goniometer measurements were prepared by grinding a plane surface on the cylindrical or bar sample. For the Debye-Scherrer method, powder was taken from the sample with a file. The powder was relieved of working stresses by annealing in an evacuated sealed quartz bulb.

### 3.5 Measurement of mechanical properties

Measurement of the ultimate tensile stress and the elongation was carried out in an Amsler testing machine.

## III RESULTS OF THE DILATATION MEASUREMENTS

### 1. DIMENSIONAL CHANGES OF THE TEST SPECIMEN DURING SINTERING

#### 1.1 Powder mixture 90W.10(2Ni.Cu)

In order to study the changes occurring at low temperatures, the test specimens were sintered in the temperature interval $500^{o}$ – $900^{o}$C. The change in diameter of the test specimens, as percentages, is shown in Fig. 6 as a function of time and temperature. Between $500^{o}$ and $600^{o}$, the test specimen begins to expand. The change has a maximum in the temperature interval $700^{o}$ – $800^{o}$C. The onset of the change, as well as its maximum, are functions of sintering time and sintering temperature.

For quantitative determination of the increase in diameter, the dimensional changes of a few specimens (green density 10.4 g/cm$^3$) were measured with the optical dilatometer. The result showed that, at least as far as experiments of long duration were concerned, that the expansion of the test specimen is a linear function of the square root of time, obeying a law of the form

1.III $$(D_s - D_0)/D_0 = k\sqrt{t}$$

The result is shown in Fig. 7. The k values for the equations are given in Table 1.

At high temperatures ($900^{o}$ – $1400^{o}$C), the dimensional changes of the compressed powder specimens were studied with the aid of the dilatometer. In this connection, test series a and b will be dealt with. The two series differ only as regards the green density of the specimen and the sintering time. The green den-

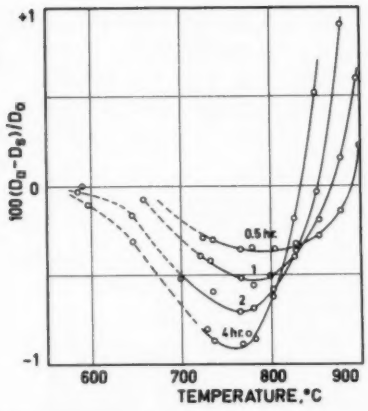


Fig. 6 Expansion of the powder cylinder at low temperatures. Mixture 90W.10(2Ni.Cu).

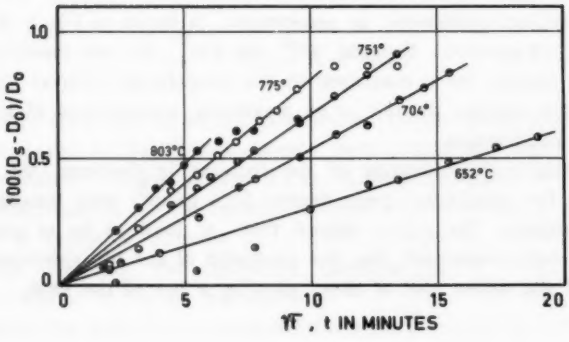


Fig. 7 Expansion isotherms at low temperatures. Mixture 90W.10(2Ni.Cu).

sity and the sintering time were 10.927 g/cm$^3$ and 240 minutes in series a, and 10.318 g/cm$^3$ and 60 minutes in series b.

Table 1.

Values of T and k,

Mixture 90W.10(2Ni.Cu).

| T<br>$^{o}C$ | k<br>$min^{-1/2}$ |
|---|---|
| 652 | $3.08 \times 10^{-4}$ |
| 704 | $5.38 \times 10^{-4}$ |
| 751 | $6.73 \times 10^{-4}$ |
| 774 | $8.04 \times 10^{-4}$ |
| 803 | $9.64 \times 10^{-4}$ |

In test series a the percentage shrinkage of diameter and height (both equal), are to be seen from Fig. 8. Closer study of the test results revealed the existence of a relationship between the change in volume of the test cylinder and the corresponding time, of the form

2.III $$\text{Log}\,[(V_o - V_s)/(V_s - V_{te})] = n\text{Log}\,k_o + n\text{Log}\,t, \text{ or}$$

$$(V_o - V_s)/(V_s - V_{te}) = (k_o t)^n$$

where $k_o$ is a rate coefficient, and n a time exponent. The index notations of the volumes (V) refer to the volume before sintering (o), during sintering (s) and after sintering into a dense compact mass (te).

For the change in diameter, a fully similar relationship was found as regards time. (The same value was obtained for n, not for $k_o$).

Fig. 9 shows the results obtained from test series a as represented in terms of the equation. The time required to insert the specimens in the furnace and for the specimen to be warmed up, usually 1 – 2 minutes, has been deducted from the sintering time (in minutes). The values of $k_o$, n and $t_o$, in accordance with equation 2.III calculated from the results of test series a, and the ultimate density ($\varrho_s$), are given in Table 2. The corresponding values derived from test series b have been compiled in Table 3.

At higher temperatures ($T>1320^{o}C$), the specimens were inserted more rapidly in the furnace in series a ($t_o<1$ minute) than in series b ($t_o>1$ minute), in order to observe the potential difference due to the presence of the liquid phase. The shrinkage results, as percentages, are to be seen from Fig. 10, and from Tables 2 and 3.

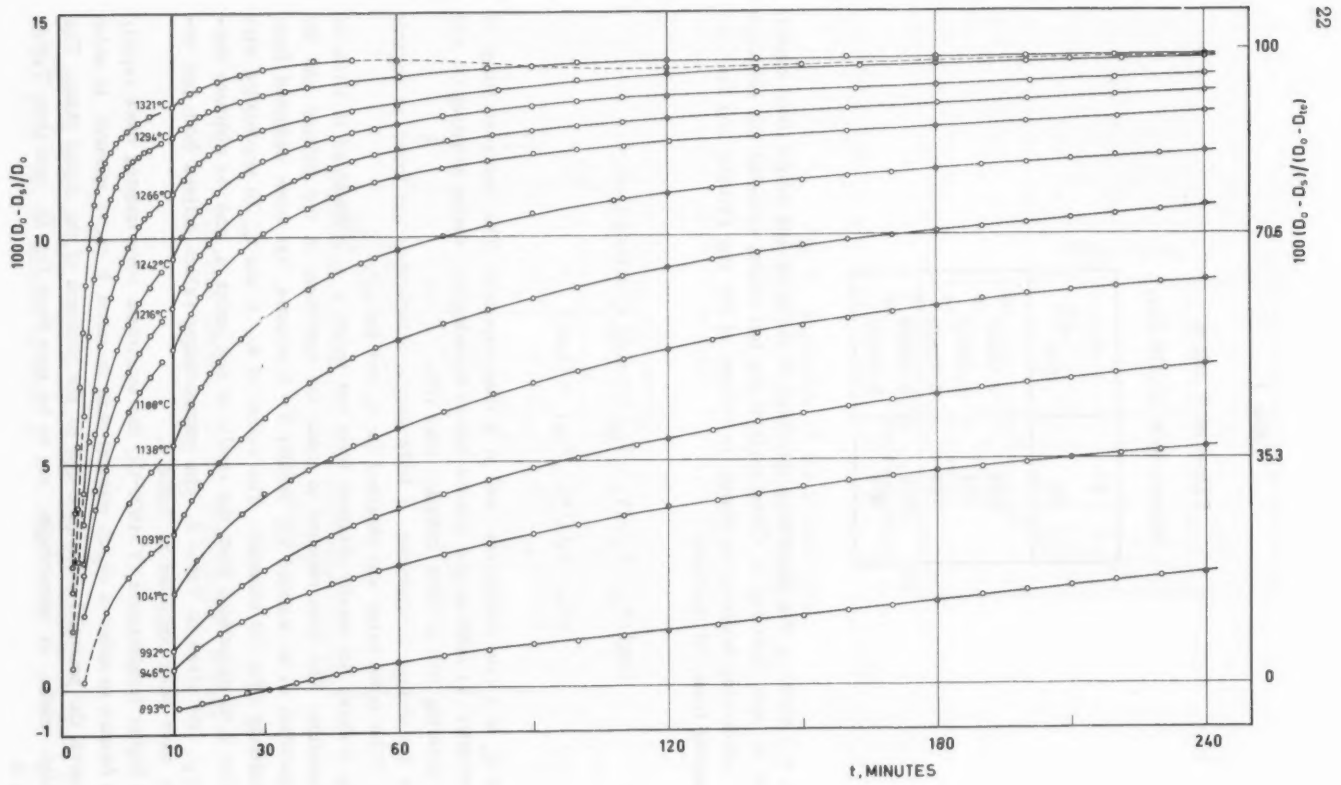


Fig. 8 Shrinkage of the powder cylinder as a function of time and temperature, Mixture 90W.10(2Ni.Cu).

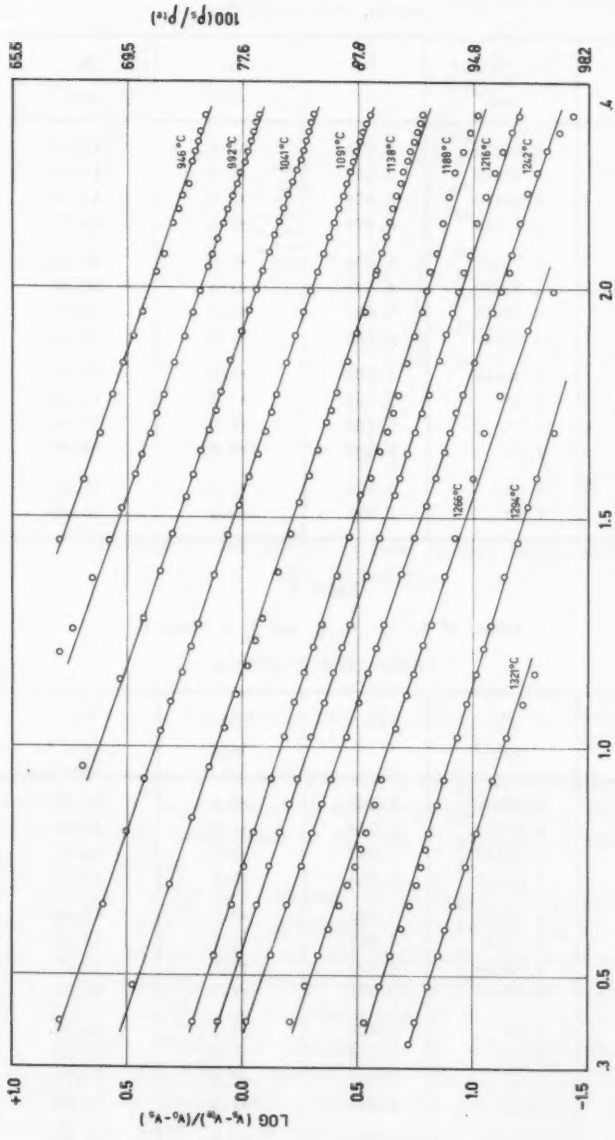


Fig. 9 Shrinkage isotherms, Mixture 90W.10(2Ni.Cu).

Table 2

Values of T, $k_o$, n, $t_o$ and $\varrho_s$ in series a,

Mixture 90W.10(2Ni.Cu)

| T °C | $k_o$ $min^{-1}$ | n - | $t_o$ min | $\varrho_s$ $gcm^{-3}$ |
|---|---|---|---|---|
| 946 | $2.54x10^{-3}$ | 0.678 | +2.0 | 12.95 |
| 992 | $5.37x10^{-3}$ | 0.683 | +2.0 | 13.61 |
| 1041 | $1.23x10^{-2}$ | 0.678 | +1.5 | 14.50 |
| 1091 | $2.77x10^{-2}$ | 0.674 | +1.5 | 15.27 |
| 1138 | $6.79x10^{-2}$ | 0.674 | +1.0 | 15.84 |
| 1188 | $1.87x10^{-1}$ | 0.635 | +1.5 | 16.30 |
| 1216 | $2.75x10^{-1}$ | 0.662 | +1.5 | 16.55 |
| 1242 | $4.29x10^{-1}$ | 0.688 | +1.5 | 16.75 |
| 1266 | $8.32x10^{-1}$ | 0.688 | +1.5 | 17.03 |
| 1294 | 2.28 | 0.688 | +1.5 | 17.18 |
| 1321 | 4.79 | 0.688 | +1.5 | 17.06 |
| 1349 | 1.53 | 1.498 | +0.8 | 16.97 |
| 1377 | 2.21 | 1.503 | +0.8 | 16.99 |
| 1402 | 2.88 | 1.502 | +0.8 | 16.93 |

Table 3

Values of T, $k_o$, n, $t_o$ and $\varrho_s$ in series b,

Mixture 90W.10(2Ni.Cu)

| T °C | $k_o$ $min^{-1}$ | n - | $t_o$ min | $\varrho_s$ $gcm^{-3}$ |
|---|---|---|---|---|
| 1103 | $2.73x10^{-2}$ | 0.635 | +0.5 | 13.78 |
| 1132 | $4.31x10^{-2}$ | 0.659 | +1.0 | 14.22 |
| 1150 | $6.01x10^{-2}$ | 0.657 | +2.0 | 14.57 |
| 1175 | $1.12x10^{-1}$ | 0.613 | +1.0 | 15.02 |
| 1205 | $1.59x10^{-1}$ | 0.620 | +2.0 | 15.48 |
| 1233 | $2.71x1($ $^{-1}$ | 0.617 | +1.0 | 15.89 |
| 1258 | $4.32x10^{-1}$ | 0.625 | +1.0 | 16.32 |
| 1287 | $9.06x10^{-1}$ | 0.631 | +1.5 | 16.74 |
| 1296 | 1.20 | 0.638 | +1.5 | 16.94 |
| 1319 | 2.58 | 0.638 | +1.5 | 17.28 |
| 1334 | 5.57 | 0.641 | +1.5 | 17.20 |
| 1350 | 9.62 | 0.694 | +1.5 | 17.22 |
| 1382 | 2.12x10 | 0.650 | +2.0 | 17.12 |
| 1406 | 4.33x10 | 0.667 | +1.5 | 17.09 |

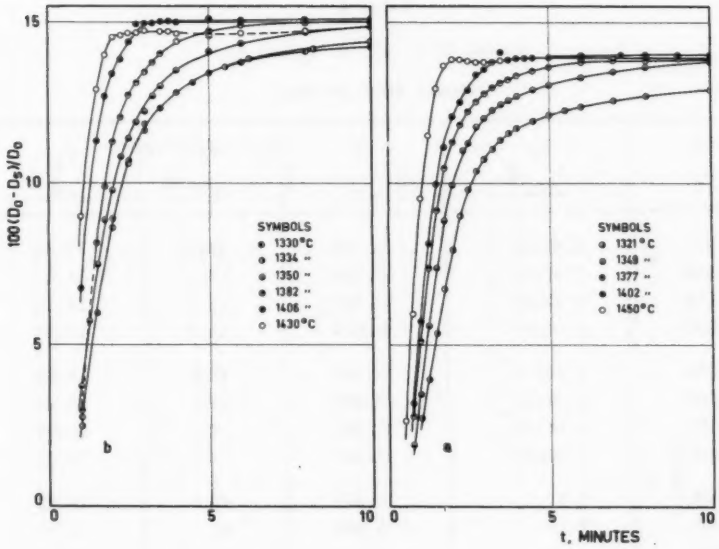


Fig. 10 Shrinkage of the powder cylinder at high temperatures, Mixture 90W.10(2Ni.Cu).

## 1.2 Powder mixtures 90W.10 Monel and 90W.10Ni

No changes occurred in the dimensions of the test specimen prepared of 90W.10 Monel powder at low temperatures. In the temperature interval 850 °C — 900 °C, the dimensions of the specimen began to decrease at the onset of sintering (duration of test 60 — 120 minutes).

The shrinkages of the test specimen during isothermal sintering at high temperatures (1100 °C — 1450 °C), as percentages, are shown in Fig. 11. The change in volume ratio, calculated from the test results as a function of time, has the form 2.III. The constant coefficients relating to this equation are given in Table 4. The test specimens had a green density of 11.074 g/cm$^3$.

The isothermal dimensional changes in the test specimens prepared from 90W.10Ni powder also obeyed equation 2.III. The measurements were performed in the temperature interval 1020 °C — 1350 °C. The sintering time was 60 minutes, and the test specimens had the green density 10.340 g/cm$^3$. The logarithmic straight line graphs here representing equation 2.III can be seen in Fig. 12, and the coefficients of the equation in Table 5.

Table 4

Values of T, $k_o$, n, $t_o$ and $\varrho_s$,

Mixture 90W.10 Monel

| T $^oC$ | $k_o$ $min^{-1}$ | n - | $t_o$ min | $\varrho_s$ $gcm^{-3}$ |
|---|---|---|---|---|
| 1117 | $2.45x10^{-2}$ | 0.596 | +4.0 | 13.84 |
| 1152 | $5.40x10^{-2}$ | 0.514 | +3.0 | 14.47 |
| 1175 | $7.48x10^{-2}$ | 0.520 | +3.0 | 14.73 |
| 1206 | $1.05x10^{-1}$ | 0.509 | +3.0 | 14.95 |
| 1234 | $1.65x10^{-1}$ | 0.467 | +2.0 | 15.09 |
| 1260 | $2.91x10^{-1}$ | 0.467 | +2.0 | 15.44 |
| 1287 | $5.26x10^{-1}$ | 0.501 | +2.0 | 15.54 |
| 1300 | $9.12x10^{-1}$ | 0.500 | +2.0 | 15.51 |
| 1320 | 1.57 | 0.509 | +2.0 | 15.72 |
| 1335 | 2.12 | 0.497 | +2.0 | 15.97 |
| 1349 | 3.17 | 0.506 | +1.5 | 16.13 |
| 1382 | 6.95 | 0.493 | +1.5 | 16.78 |
| 1406 | 1.42x10 | 0.502 | +1.0 | 17.03 |
| 1430 | 1.98x10 | 0.506 | +1.5 | 16.94 |

Table 5

Values of T, $k_o$, n, $t_o$ and $\varrho_s$,

Mixture 90W.10Ni

| T $^oC$ | $k_o$ $min^{-1}$ | n - | $t_o$ min | $\varrho_s$ $gcm^{-3}$ |
|---|---|---|---|---|
| 1020 | $1.12x10^{-2}$ | 0.845 | 0 | 12.44 |
| 1119 | $6.20x10^{-2}$ | 0.792 | +1.0 | 14.61 |
| 1150 | $1.07x10^{-1}$ | 0.788 | +1.0 | 15.24 |
| 1177 | $1.70x10^{-1}$ | 0.771 | +1.0 | 15.70 |
| 1212 | $3.20x10^{-1}$ | 0.773 | +1.0 | 16.09 |
| 1249 | $5.54x10^{-1}$ | 0.782 | +1.0 | 16.43 |
| 1273 | $6.69x10^{-1}$ | 0.788 | +1.0 | 16.44 |
| 1300 | $9.10x10^{-1}$ | 0.851 | +1.0 | 16.69 |
| 1350 | 1.24 | 0.820 | +0.5 | 16.78 |

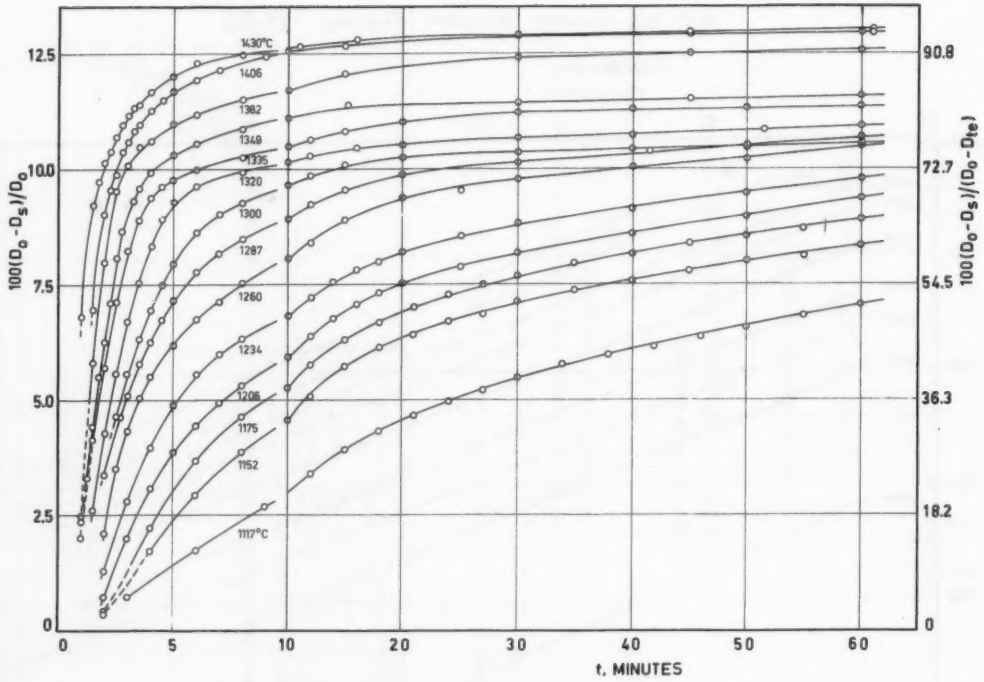


Fig. 11 Shrinkage of powder cylinder as a function of time and temperature, Mixture 90W.10 Monel.

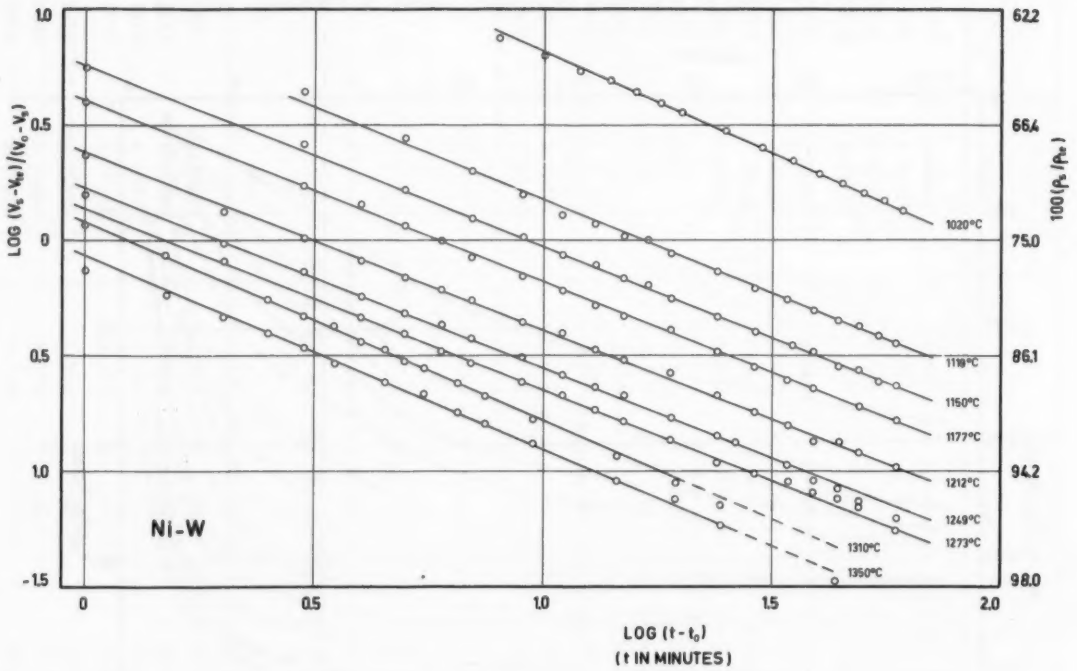


Fig. 12 Shrinkage isotherms, Mixture 90W.10Ni.

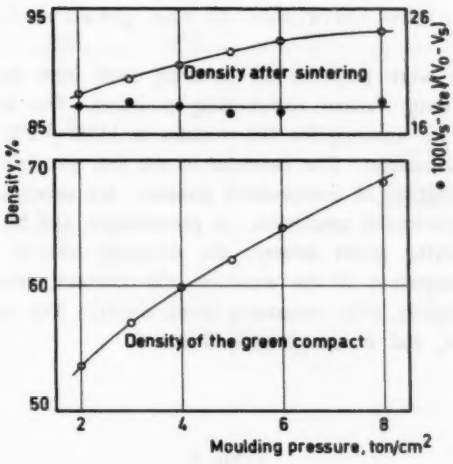


Fig. 13 Density of the powder cylinder before and after sintering, as a function of compression.

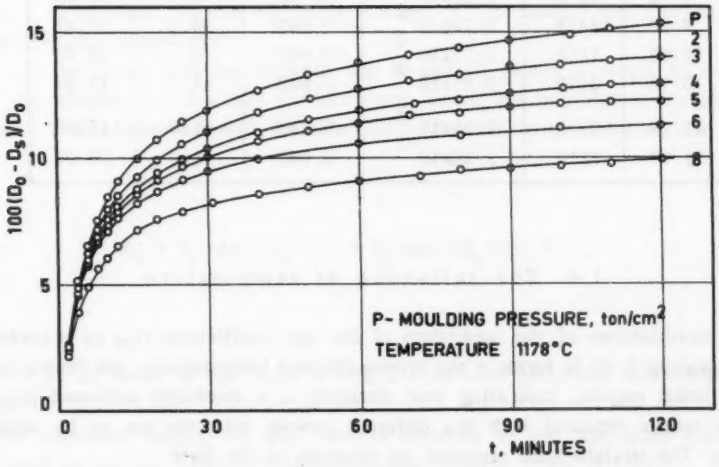


Fig. 14 Shrinkage of the powder cylinder as a function of time and compression.

## 1.3 The influence of the green density

Test specimens were prepared for sintering tests from the 90W.10(2Ni.Cu) powder mixture, using various compressing pressures. The dimensional changes in the specimens on sintering for 120 minutes at $1178^{o} \pm 1^{o}C$ were studied with the aid of the dilatometer. The densities of the test specimens before and after sintering, as a function of compression pressure, are shown in Fig. 13, and the dimensional changes in the specimens, as percentages, can be seen from Fig. 14.

Despite the varying green density, the shrinkage obeyed sintering equation 2.III. The time exponent of the equation was constant, while the rate coefficient increased slightly with increasing green density. The calculated values of the constants $k_o$, $t_o$ and n are given in Table 6.

Table 6

Values of T, $k_o$, n, $t_o$ and $\varrho_s$ for varying green density $\varrho_o$.

Mixture 90W.10(2Ni.Cu)

| $\varrho_o$ $gcm^{-3}$ | T $^{o}C$ | $k_o$ $min^{-1}$ | n - | $t_o$ min | $\varrho_s$ $gcm^{-3}$ |
|---|---|---|---|---|---|
| 9.25 | 1178 | $1.20 \times 10^{-1}$ | 0.643 | +2.0 | 15.23 |
| 9.83 | 1178 | $1.15 \times 10^{-1}$ | 0.643 | +1.3 | 15.44 |
| 10.33 | 1178 | $1.17 \times 10^{-1}$ | 0.643 | 0 | 15.65 |
| 10.70 | 1178 | $1.25 \times 10^{-1}$ | 0.643 | +1.5 | 15.81 |
| 11.15 | 1178 | $1.23 \times 10^{-1}$ | 0.643 | +1.0 | 15.95 |
| 11.77 | 1178 | $1.16 \times 10^{-1}$ | 0.643 | +1.0 | 16.09 |

## 1.4 The influence of temperature

On examination of the logarithms of the rate coefficients ($k_o$) in accordance with equation 2.III in terms of the inverse absolute temperatures, one finds a number of linear regions, indicating that sintering is a thermally activated process.

The results obtained with the different powder mixtures are to be seen in Fig. 15. The straight lines represent an equation of the form

3.III $$k_o = k_i \exp(-Q_i/RT)$$

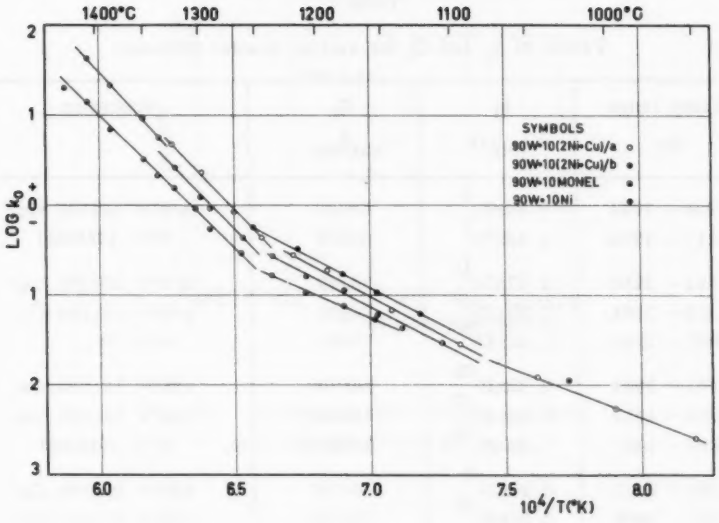


Fig. 15 Temperature-dependence of the sintering rate coefficient.

where $k_i$ is constant, $Q_i$ the activation energy, R the general gas constant and T the absolute temperature.

It can be noted from the diagram that $k_i$ and $Q_i$ values different in magnitude are obtained in one and the same test series, but in different temperature regions. The relation between the rate coefficient and temperature is thus

4.III $$k_o = k_1 \exp(-Q_1/RT) + k_2 \exp(-Q_2/RT) + \ldots\ldots,$$

where one or other of the terms is effective in each particular temperature interval.

The transition ranges, if any, always occurred in the test series studied in this work in one and same temperature range, namely, $1050^o$ — $1100^oC$, $1200^o$ — $1250^oC$, $1300^o$ — $1350^oC$ and $>1400^oC$.

The $k_i$ and $Q_i$ values for the different ranges of temperature are given in Table 7.

Table 7

Values of $k_i$ and $Q_i$ for various powder mixtures

| Temp. range °C | $k_i$ $min^{-1}$ | $Q_i$ cal/mol | Specimen - |
|---|---|---|---|
| 946 ··· 1041 | $9.24 \times 10^{6}$ | 55300 | a/90W.10(2Ni.Cu) |
| 1117 ··· 1234 | $4.48 \times 10^{7}$ | 58100 | 90W.10Monel |
| 1091 ··· 1216 | $2.07 \times 10^{10}$ | 74100 | a/90W.10(2Ni.Cu) |
| 1103 ··· 1205 | $1.29 \times 10^{10}$ | 73800 | b/90W.10(2Ni.Cu) |
| 1020 ··· 1249 | $8.40 \times 10^{9}$ | 70900 | 90W.Ni |
| 1242 ··· 1321 | $6.22 \times 10^{20}$ | 146700 | a/90W.10(2Ni.Cu) |
| 1233 ··· 1319 | $6.28 \times 10^{20}$ | 148500 | b/90W.10(2Ni.Cu) |
| 1260 ··· 1430 | $7.30 \times 10^{18}$ | 136100 | 90W.10Monel |
| 1349 ··· 1402 | $8.20 \times 10^{8}$ | 64700 | a/90W.10(2Ni.Cu) |
| 1330 ··· 1406 | $3.25 \times 10^{21}$ | 152700 | b/90W.10(2Ni.Cu) |

## 2. A QUALITATIVE DISCUSSION OF SINTERING

On the basis of the results now obtained, it is possible, to begin with, to make a qualitative study of the mechanism of sintering as far as the investigated powder mixture is concerned. For the purposes of this discussion, we shall divide the sintering range into several individually distinct temperature intervals according to the observed changes, as follows: Range A: 500° ··· 900°C, Range B: 900° ··· 1083°C, Range C: 1083° ··· 1250°C, Range D: 1250° ··· 1400°C, Range E: >1400°C. Fig. 16 shows schematically the change of density in the various temperature ranges when the sintering time amounts to several hours. The influence of short treatment times and of temperature upon loose 90W.10(2Ni.Cu) powder was qualitatively studied by means of the emanation technique. The measuring equipment was nearest to the type employed by Schreiner (ionization chamber, amplifier, galvanometer) [43]. The sample was marked with radioactive thorium nitrate solution (surface activity about 0,03 mC) and dried. The thorium emanation discharged by the sample was led into the ionization chamber with the protective gas (hydrogen). During measurement, the rate of temperature increase was about 8° ··· 9°C per minute. The result of two measurements is shown in Fig. 17. The measurements are mutually different only in that the increase in temperature was stopped in the case of one sample (1a) for three hours at 900°C for the purpose of isothermal measurements, while the measurement was carried on without interruption as regards the other sample (1b).

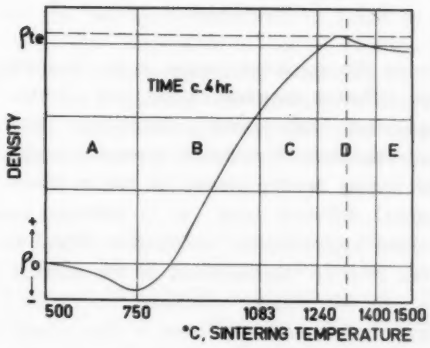


Fig. 16 Density of the powder cylinder as a function of temperature.

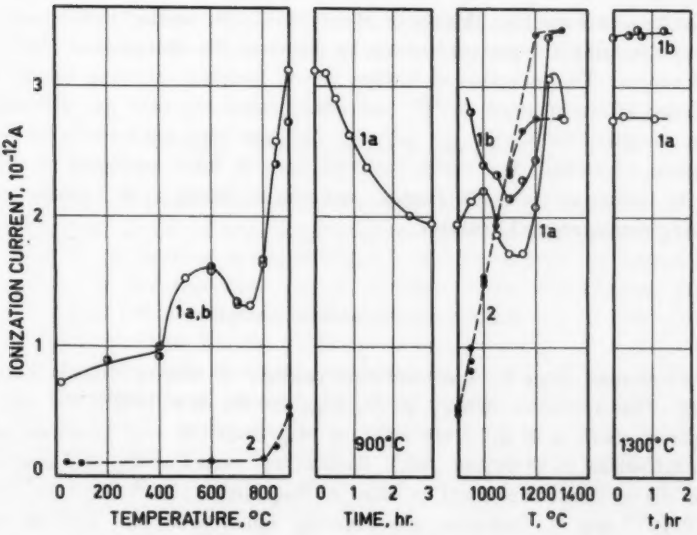


Fig. 17 Diffusion of emanation as a function of time and temperature.

## 2.1 Temperature range A

The first changes in the specimen begin in the temperature interval 500°... 600°C, owing to the diffusion between coppar and nickel. The point of onset of changes is in agreement with previous observations [33]. In the dimensions of the test specimen, the onset of diffusion is seen as a slight decrease in density. The change in density in the system is not a direct consequence of the difference of the partial diffusion rates, as in diffusion contact tests the total volume remains at least approximately unchanged (Seith [44]). In powder systems, it is rather the relative displacement of the contact pairs (Cu/Ni) which produces this change, in the manner described by Bückle [45] among others. The dimensional change in the test specimens is thus related to the overall diffusion constant (not directly to the partial diffusion constants). The result in accordance with equation 1.III can thus be derived on the basis of the simple diffusion theory. Since the result is only qualitative in character, it will not in this connection be treated in more detail. However, it may be mentioned that the activation energy obtained from the rate coefficients (about 30 kcal/mol) is correct as to its order of magnitude (Mehl [46]). The density of the specimen attains a minimum at about 750°C, after which it begins to increase as a result of sintering.

It can be seen from Fig. 17 that at about 400°C the emanation-discharge capacity of the sample begins to increase by reason of the strengthened lattice motion of copper. The reduction of surface due to incipient sintering outweighs the temperature effect at about 600°C, and consequently the rare gas diffusion decreases. At about 750°C, the gas diffusion increases once again owing to the lattice motion of nickel. The result obtained here is fully analogous to that obtained by Schreiner [43] for copper, and also to Hüttig's [47] theory for corresponding temperatures ($\beta$ theory).

## 2.2 Temperature range B

In temperature range B, a considerable increase of density already occurs in sintering. The activation energy of shrinkage for the 90W.10(2Ni.Cu) and 90W.10 Monel mixtures is of the same order of magnitude (55 ... 58 kcal/mol) as that for the self-diffusion of copper [46]. Further, the values of the rate coefficients ($k_o$) for the mixtures are equal in order of magnitude (1000°C: $4.7 \cdot 10^{-3}$ $min^{-1}$ and $2.9 \cdot 10^{-3}$ $min^{-1}$). However, the sintering equations of the mixtures cannot be immediately compared in any other respect since, primarily for reasons which are geometrical in nature, the time exponents are different in magnitude. As one of the two powders already contained copper and nickel in an alloyed state, which was not the case for the other one, it appears, at any rate from the standpoint of qualitative assessment, as if the Cu/Ni diffusion would not affect the mechan-

ism of sintering (cf. the analogous statements of Butler et al. [30] and Duwez et al. [26, 31]). It is also impossible to assume that the Cu/Ni alloying takes place at such a high rate in the temperatures concerned [33, 34] that the shrinkage result is from the very beginning representative of the completed alloy. One explanation of the result now obtained can obviously be derived from the approximate equality as regards absolute values and activation energies of the self-diffusion rates of pure copper as well as the copper in the mixture (cf. paragraph 3.5).

In addition to the Cu/Ni diffusion, the dissolution of tungsten in the mixture has an effect in this range, which is indicated by the fact that Curie temperatures decreased permanently to a level below room temperature. The Curie temperature of the (2Ni.Cu) alloy is 27°C [33]. Since the Curie temperature of the 90W.10 Monel mixture does not decrease to any noteworthy extent in this range (Fig. 18), one has in this instance to assume that dissolution of tungsten as well as of copper in nickel takes place. (The influence of tungsten upon the Curie point of nickel is about twice that of copper [34]).

In the emanation experiments (Curve 1a) a corresponding decrease in gas diffusion with isothermal sintering (at 900°C) can be noted. When the temperature is subsequently raised, an increase of diffusion becomes evident (incipient lattice motion of tungsten). In the experiment without isothermal sintering (Curve 1b), also there can be seen a decrease in emanation discharge attributable to sintering, though it is not so marked as in the preceding instance. In both cases, the minimum of emanation diffusion lies in the melting point region of copper.

## 2.3 Temperature range C

In the case of the 90W.10(2Ni.Cu) powder mixture a change in the sintering mechanism occurs in the neighbourhood of the melting point of copper, as manifested by an increase in the shrinkage activation energy (74 kcal/mol). The value found for the activation energy is close to the self-diffusion activation energy of nickel (66.8 kcal/mol Hoffman et al. [49]). For the 90W.10Ni mixture, a value is found for the shrinkage activation energy (71 kcal/mol) which is also of the same order of magnitude as that for the self-diffusion of nickel and for the interdiffusion of tungsten (in dilute solution) in nickel (77 kcal/mol, Swalin et al, [50]). As for the 90W.10Monel mixture no change occurs in this range in comparison with the preceding range. In the light of these results, it seems obvious that the sintering of the 90W.10(2Ni.Cu) powder mixture is primarily governed by the self-diffusion of nickel, insofar as interdiffusion does not affect the result (the diffusion rate of tungsten in nickel is lower than that of nickel [49, 50]). It is very hard to explain the result obtained in any way other than by the assumption that for one reason or another the influence of copper becomes less. In any other case, the sintering would have to occur in a manner equivalent to that of the 90W.10Monel mixture ($Q \sim 58$ kcal/mol).

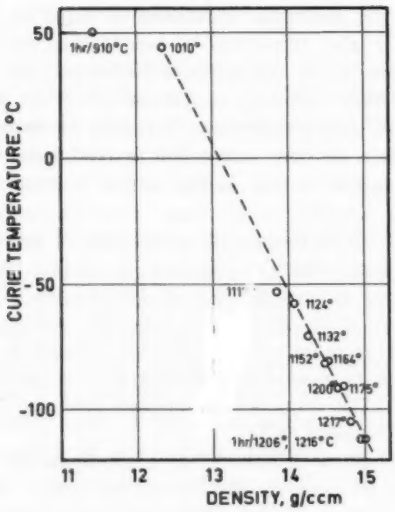


Fig. 18 Curie temperature of the sintered specimen as a function of density.

This influence of copper on the sintering mechanism is not yet clear. Obviously the melting of copper is involved in some way or other, as according to the present results, the change of mechanism of sintering occurs immediately following the melting point of copper. One might assume that copper is eliminated primarily through the agency of surface adsorption. (According to published results, molten copper wets tungsten but not nickel, from which follows its adsorption by the tungsten surfaces; Parikh [51], Bondi [51]. The mixture would then present an analogy to the behaviour of the WC/Co mixture at the melting point of cobalt; Baxter et al. [52]. Small quantities of nickel dissolved in the molten copper might act as boundary surface-active agents, facilitating the wetting; Livey et al. [30], Boos [53]). However, the observations relating to the sintering of W/Cu contact mixtures and others are not in support of this assumption where low-temperature is concerned; on the other hand, again, the observations reported in publications are so far in disagreement, and on this basis it will hardly be possible to clarify the matter.

Slight alloying in the material does not greatly alter the self-diffusion of the base material. On the basis of the few investigations carried out in this field, it can be noted that impurity may cause changes in the value of the self-diffusion rate and of its activation energy (Gruzin [54], Hoffman et al. [55], Swalin et al. [50]). In the case investigated, it can be assumed that tungsten

has an effect of increasing the self-diffusion energy of nickel (cf. the analogon of the Fe-Cr system [54]).

In the case of the 90W. 10Monel powder mixture, there occurred strong diffusion of tungsten into the Monel powder in this temperature range. The result of the Curie temperature determination can be seen in Fig. 18, where the Curie temperature has been plotted against density (note the analogy with Torkar's observations [33]). The sintering temperatures corresponding to the measured points have also been entered in the figure; they show that, with one and the same time of treatment, interdiffusion is not solely dependent upon temperature. In this case, too, interdiffusion does not seem to affect the course of sintering to any noteworthy extent.

According to Fig. 17, the emanation diffusion begins to increase above 1150°C in either sample. In isothermal sintering carried out at 1300°C, the emanation diffusion no longer decreases in correspondence with the sintering of tungsten. On cooling the sample, there is obtained a definite emanation discharge curve dependent on temperature. As the measured values thus represent the thermal equilibrium of emanation diffusion, the activation energy of gas diffusion can be derived from the temperature dependency of the curve. It has a value of about 35 kcal/mol in the temperature interval 800° ··· 1000°C. This value is of the same order of magnitude as the activation energy of rare gas diffusion in oxide systems (e. g. $UO_2$/Xe; Q = about 40 kcal; Lindner [56]), and it thus exceeds considerably the corresponding values given for metals by Schreiner [43]. It can therefore be assumed that curve No. 2 does not represent the emanation diffusion in the lattice of a dense metal mixture alone (the obtained values are too large also in comparison with the diffusion surface to be real) but that it also includes the emanation diffusion in the thorium oxide partially discharged on compaction of the sample. (cf. the analogy: when tungsten is being sintered, the major part of the oxide and silicate additions come out as the specimen becomes more compact; e. g. Nachtigall [57]).

## 2.4 Temperature range D

A change again occurs in the mechanism of sintering with the powder mixtures 90W. 10(2Ni. Cu) and 90W. 10Monel at a temperature of about 1250°C. The activation energy values for sintering (136 ··· 148 kcal/mol) are approximately the same as for the self-diffusion of tungsten (135. 8 kcal/mol, Wasiljev [58]). The point of change lies in the temperature range in which the lattice motion of tungsten becomes stronger (60 ··· 80 minutes are required for the commencement of recrystallization at 1250°C, Nachtigall [57]).

It can be assumed that during the warming up of the test specimen the Cu/Ni phase is already sintered at such a high rate, and to such an extent, that the tungsten grains touch each other, and continued change without any effect from the tungsten is impossible. A corresponding phenomen is observable, for instance,

in Cr-$Al_2O_3$-cermet (Onitsch-Modl [30]), where the sintering of the chromium powder takes place in the temperature interval 1350° ··· 1450°C. If the temperature is not raised, the densification of the compact will stop at this stage. In the temperature interval 1550° ··· 1650°C, the final sintering of cermet occurs through the effect of cation diffusion. In the mixture investigated, conditions are more favourable than in the preceding instance, in that tungsten may move through the binder phase, thus facilitating the process of sintering. One may therefore assume that approcimately theoretical density will be obtained with the powder under investigation within relatively short treatment times and at low temperatures, which determine the incipient lattice motion (result: sintering 10h/1245°C; green density 10.3 g/$cm^3$ and obtained density 17.23 g/$cm^3$).

The pure (2Ni.Cu) phase has a melting point of 1320°C. If the test specimen is heated very rapidly to above this temperature, melting of the phase will be possible because its melting point has not time to rise sufficiently, owing to the slow tungsten diffusion. The sintering mechanism then changes, because macroscopic flow partially replaces the diffusion flow. This is noticed, for instance, as a change of the time exponent and of the activation energy (Tables 2, 3 and 7). The values in the tables can be considered to be qualitative in this case only, because the high sintering rate prevents the making of accurate observations. If the sintering is effected in such a manner that the diffusion of tungsten into the binder phase prevents its melting, the sintering mechanism will remain the same as that at low temperatures.

## 2.5 Temperature range E

When the temperature is sufficiently high, the increasing solution of tungsten in the Ni-Cu-W phase no longer hinders the melting of the phase (Price et al. [59]). At these temperatures, the sintering mechanism changes permanently into a macroscopic flow induced by the surface forces (for theory, see: Lenel, Lenel and Cannon et al. [60]). The condition can then be likened to the phenomena occurring between wetting bonding metals and oxides, carbides, borides, etc. (e.g. Ag-Cu/$Al_2O_3$, Baxter [52]; Co/WC, Cu-Ni/ZrC etc., Livey and Murray [61]).

In actual practice, this temperature range (or generally the temperatures above the melting point of pure Cu-Ni phase) can be considered an over-sintering range. However, heavy metal alloys are also manufactured in this manner (entirely in the U.S.A. and England). Grain growth is prevented by means of a short sintering time (0.5 h/1420°C). It should be noted that an over-sintered product is inferior in its density and mechanical properties, owing to precipitations (Green [62]; tungsten dissolved in the matrix) and other reasons.

# 3. A QUANTITATIVE DISCUSSION OF THE SINTERING

## 3.1 The deduction of a new sintering equation

In ideal sintering models with a simple geometry, the decrease in volume occurring on sintering has the form [8, 10, 21)

5. III $$(V_o - V_s) / V_o = k' t^n$$

Writing $(V_o - V_s) / (V_o - V_{te}) = \alpha$ we find the equation

6. III $$\alpha = [V_o / (V_o - V_{te})]\, k' t^n = k t^n$$

where $V_o$, $V_s$ and $V_{te}$ are respectively the volumes of the specimen subjected to sintering before and during sintering, and after having been sintered to a dense state, while k is a rate coefficient and n a time exponent.

A differentiation of equation 6. III yields the rates of change in the volume of the specimen and in the porous volume fraction:

7. III $$-dV_s / (V_o - V_{te})\, dt = n k t^{n-1} = d\alpha / dt$$

The ideal model is valid only in a given sintering range, that is, as long as the contact area between the powder grains is small. An attempt will consequently be made to find, on the basis of our results, a sintering equation which is applicable in the entire sintering region.

Let us assume that when the contact area grows large, a rate equation of the same form (7. III) is applicable, but that in addition the factors retarding the process, resulting from the change in geometry of the matrix and from the interaction of the growing contacts, will have their influence. We assume that these factors are proportional to some power (i) of the residual sintering fraction, or to what is termed the impingement factor $(1 - \alpha)^i$. The new rate equation, in terms of the change in volume, will then have the form:

8. III $$-dV_s / (V_o - V_{te})\, dt = n [(V_s - V_{te}) / (V_o - V_{te})]^i k t^{n-1}$$

Integration of equation 8. III yields

9.III $$(V_s - V_{te})^{1-i} / (1-i) = -(V_o - V_{te})^{1-i} kt^n + I, \quad (i \neq 1)$$

For $t = 0$, $V_s = V_o$ and $I = (V_o - V_{te})^{1-i} / (1-i)$, and the ultimate solution thus has the form

10.III $$\left[(V_s - V_{te})/(V_o - V_{te})\right]^{1-i} = 1 - (1-i)kt^n, \quad (i \neq 1)$$

Solving for the ratio $\alpha$, we find

11.III $$(1 - \alpha)^{1-i} = 1 - (1-i)kt^n, \quad (i \neq 1)$$

$$(1 - \alpha) = \exp(-kt^n), \quad (i = 1)$$

When a substitution is made in equation 11.III of the results corresponding to the temperature of 1091°C from the sintering experiment (Figs. 8 and 9), the result shown in Fig. 19 is obtained. It can be seen that, with increasing impingement exponent i, there is an improvement in the fit of the experimental plots with straight lines, up to the value i = 2, after which the fit again becomes poorer.

From the linear sections of the curves in Fig. 19, the constant coefficients of the equations can be determined as functions of the impingement exponent. The region of validity of the curves and the constants of the equations have been compiled in Table 8. Between the impingement exponent i and the time exponent n, there exists in this instance an approximate linear relationship of the form

12.III $$n = 0.49 + 0.10i$$

Table 8
Constants of the sintering equation

| Impingement exponent | 0 | ½ | 1 | 1½ | 2 | 2½ |
|---|---|---|---|---|---|---|
| Rate coefficient, k | 0.095 | 0.093 | 0.091 | 0.091 | 0.090 | 0.087 |
| Time exponent, n | 0.489 | 0.536 | 0.583 | 0.623 | 0.672 | 0.733 |
| Range of validity of the equation | | | | | | |
| 0 - $t_s$, min | 18 | 20 | 25 | 60 | 240 | 35 |
| 100 ( $\alpha_s / \alpha_{240}$) | 48 | 50 | 55 | 75 | 100 | 63 |

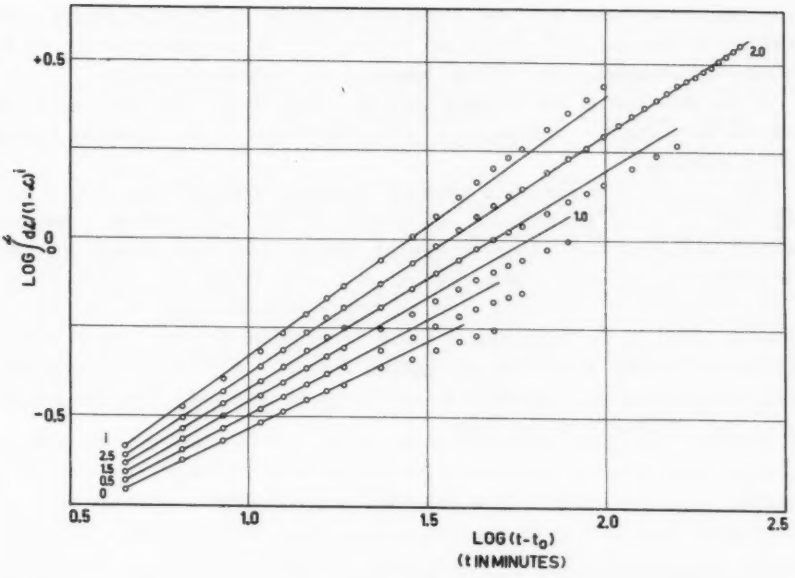


Fig. 19 Shrinkage isotherms for different values of the impingement factor.

## 3.2 The impingement factor

The shrinkage of the specimen subjected to sintering is caused by the growth of the contacts between the powder grains at the expense of the grains. With progressive sintering, conditions are changed in the contacts as well as in the matrix, and the result is a reduction of the sintering rate.

The sintering in the late stages is retarded for reasons which include the following:

- The growing contact areas collide, and their growth stops, or is slowed down along their area of collision,
- In the course of growth of contact areas and, in later stages of grains, the free surfaces and grain boundaries, which act as vacancy sources and sinks, decrease [10, 17, 18, 20], resulting in a reduced sintering rate,
- The high sintering rate of the earliest stages of sintering, probably resulting from extensive sliding motions of the grain boundaries, abates to its normal value as determined by diffusion [63].

- The active states that have come into existence in the initial stages of the sintering of one and multi-component systems [37, 38] disappear through the influence of homogenization, and the sintering rate consequently drops.

In the deduction of the sintering equation, these factors have been taken into account by taking the sintering rate to be proportional to the remaining fraction of the sintering.

This method of treatment is common in kinetic considerations of solid state reactions, e. g. of precipitation and decomposition transformations. Assuming random nucleation in precipitation kinetics, Avrami [64] and Johnson and Mehl [65] find, for the approximate reaction of a large number of grains, the impingement factor $(1 - \alpha)$, which is in conformity with the results of experiment. However [66], as the impingement factor compensates for a number of effects, one has to assume that it has the general form $(1 - \alpha)^i$, in which exponent i obtains various values, dependent on the factors of influence. Thus the precipitation equation will have the form

$$13.\text{III} \qquad \text{Log} \int_0^{\alpha} d\alpha \,/\, (1 - \alpha)^i = \text{Log } k + n\text{Log } t$$

In precipitation kinetics, Lement and Cohen [66] (the first stage of tempering in steel) find a linear relationship in accordance with equation 13. III in the region $\alpha = 0$ and $\alpha = 0.5 \pm 0.1$, with an impingement exponent varying between $i = 0$ and $i = 2$. The time exponent was only slightly variable as a function of the impingement exponent.

Equation 8. III relates to integration of the equation 13. III. In the present investigation, the linear relationship stated by equation 13. III manifested itself in full strength, with the impingement exponent equal to 2. In precipitation kinetics, the value $i = 2$ has been found more suitable than Avrami's value $i = 1$ in quite a number of cases (Austin and Ricket [67], Hickley and Woodhead [68], etc.). When several factors which retard a reaction are simultaneously active, it is extremely difficult to determine the value of the impingement factor by an analytical method. According to publications, the impingement factor has been mathematically analyzed in only very few cases (Mampel [69], Lement [66]).

## 3.3 The time exponent

With the ideal models, the time exponent of the sintering equation varies in accordance with the diffusion equation of the adopted model and its solution. When bulk diffusion is the principal mechanism, varying values within the range of 0.4 ··· 0.8 have been obtained for the time exponent [8, 10].

In the case of technical powders, in which the grains are not mutually equal in size and shape, the magnitude of the time exponent is determined by kinetics, in all probability by the geometry of the grains as well [21]. In investigations that have been carried out, varying exponent values have been found, dependent upon the sintering equation and upon the kind of the powder and its pretreatment. Treatment of the results in accordance with equation 3.I yields, in the initial stages of sintering for the pure component specimens, exponent values varying between 0.2 and 0.4 [22 ··· 24]. By equation 4.I, correspondingly, exponents between -0.5 and +0.5 are obtained, dependent on temperature and time [25]. In oxide systems, in which the bulk diffusion mechanism is similarly assumed to dominate, exponents of a magnitude between 0.1 and 0.4 are obtained when equations corresponding to the ideal models are applied (e.g. Coble [10], Quirk [70]).

In the present work, the time exponent varies within the range of 0.5 ··· 1 with the one-component as well as the multi-component compacts; however, it is constant with regard to temperature and time in one and the same system. The time exponent corresponding to the ideal model is obtained when the impingement exponent is zero. According to equation 12.III, the time exponent is thus about 0.5 and it is thus seen to fall within the range predicted by theory.

## 3.4 The rate coefficient

The rate coefficient of equation 5.III for ideal models has the form [10, 8]

14.III $$k' = F(N)\left[B\,\gamma\, a^3 D_d / R^m kT\right]^n$$

where F(N) is a function of the number of contacts per particle, $a^3$ is the volume of one vacancy, in $cm^3$, $\gamma$ the surface energy, in ergs per $cm^2$, $D_d$ the self-diffusion constant of the material, in $cm^2/s$, R the grain radius, in cm, k Boltzmann's constant = $1.38 \cdot 10^{-6}$ ergs per degree, n the time exponent, T the absolute temperature in $^oK$, and B a numerical coefficient.

On mutual comparison of the different sintering models, they are found to differ mainly only as regards their different numerical coefficient and time exponent.

The equation of the ideal models is valid only until the growing contacts collide. In a hexagonal tight packing, for instance, even a linear shrinkage by four per cent causes collision, while in an open cubic packing the shrinkage may be much greater before collision occurs. (It has been assumed that the contact necks act as vacancy sources, and the grain boundaries as points of vacancy destruction [10]).

It was assumed in the derivation of the sintering equation that a rate equation of ideal form is valid, and the rate coefficient (equation 6.III) is thus $k = \left[V_o / (V_o - V_{te})\right] k'$. Examination of the application (Table 8) reveals that the rate coefficient becomes slightly smaller with an increasing impingement exponent. The rate coefficient obtained from the ideal models can thus be used, qualitatively at least, in assessing the sintering rate for technical powders. As the rate coefficient implies a spherical grain, not a distribution of non-spherical grains, it can be assumed that equation 14.III, applied to the mean grain size, will give results which are too small. When the packing contains grains of different sizes, the number of contacts is higher and more difficult to assess (self-sieving and other effects) than in the case of a regular packing. When the grain is irregular, there may be contact areas instead of contact points, and the diffusion surface may become much larger than that obtained by calculation, even if the grain distribution is quite narrow.

On sintering electrolytic copper powder, the grain distribution of which is shown in Fig. 1, the following sintering equation was found (time in minutes):

15.III $$\alpha / (1 - \alpha) = \left[t \times 1.67 \cdot 10^{8} \exp(-46000/RT)\right]^{0.62}$$

Employing the ideal sintering model of Kingery and Berg [8], the value $k = 1.2 \cdot 10^{-2}$ (1/s) is obtained for the rate coefficient at 1000°C (equation 14.III). The following values were used in calculating this result: B = 80, $\gamma$ = 1700 ergs per $cm^2$, F(N) = 3N/8, N = 9.8, $R = 5.5 \cdot 10^{-4}$ cm, m = 3, $\varrho_o$ = 6.14 g/$cm^3$, $D = 4.1 \exp(-54000/RT)$ $cm^2/s$, and T = 1273°K. The empirical value computed from equation 15.III is $k = 3.5 \cdot 10^{-2}$ (1/s). When these results are compared, one finds that there is a very small difference between observed and calculated value, despite the difficulty of estimating the contact number. [71]

## 3.5 The diffusion constant of the sintering equation

In deduction of the sintering equation, the diffusion was assumed to govern the rate of sintering. According to the diffusion model, it is mainly bulk diffusion that produces changes in the dimensions of the powder specimen, and the diffusion constant should therefore be in correspondence with bulk diffusion. However, surface and grain boundary diffusion may indirectly affect the result when the grain size is small, in which case grain boundaries and surfaces are abundantly represented in the system. The sintering rate will then increase, and usually the activation energy also diminishes, so that, particularly at low temperatures, considerable differences in temperature dependence can be observed, as

compared with bulk diffusion [5, 48]. The influences of plastic deformation, torsion, pressure, etc., possibly induced by the pressure and surface forces, may alter the sintering rate by affecting the diffusion constant (Darby and Tomizuka [72], Nachtrieb [73], Hauffe [48], Jones [63], etc.).

In multi-component systems, it is extremely difficult to determine the effective diffusion constant because there are many factors influencing it.

On sintering ready-alloyed metal powders, the rate is probably determined by the self-diffusion constant of the component having the lowest rate of diffusion. Analogously, in numerous oxide systems (ionic lattice), cation self-diffusion is slowest, and therefore determines the sintering rate and the activation energy [10, 56, 70]. In the present work, this case is represented by the sintering of Monel (90W.10Monel). One can assume, on the strength of the activation energy, that the component diffusing at the slowest rate is copper. This appears plausible if one considers the atomic size effect [37], the copper concentration of the mixture, and the melting point effect, as agents accelerating the diffusion of nickel [46]. Thus, the interdiffusion of tungsten does not seem to affect the result in this instance, except perhaps by increasing the activation energy for the self-diffusion of copper (W and/or Ni) [54, 55].

When the material components are separate in the powder, there also simultaneously occurs interdiffusion in addition to sintering. In the case of the investigated (90W.10(2Ni.Cu)) mixture, this instance is represented by the investigated range. If the alloying of the (2Ni.Cu) mixture on sintering is assumed to take place very rapidly ($T < 1083^{\circ}C$), this case will be analogous to the sintering of Monel, and the self-diffusion of copper in the mixture will determine the process. It is likely that copper governs the sintering processes even if the alloying occurs slowly, for the reason that (pure) nickel cannot participate significantly in the process, owing to its low self-diffusion rate ($1000^{\circ}C$: $D_{Ni} = 4.3 \cdot 10^{-12}$ and $D_{Cu} = 2.2 \cdot 10^{-9}$ $cm^2/s$ [49, 46]; nickel thus displays an analogy with tungsten).

Although interdiffusion does not seem to have any great immediate effect upon sintering, its indirect significance with regard to the rate and continuity of sintering may be highly important. Through its influence, those highly active states of faulty order come into being which guarantee the formation (and the destruction) of lattice vacancies and their sufficient number and rate. This is the basis of the action of numerous sintering catalysts (Jones et al. [38], Layden [38], Thümmler [37], etc.). The favourable (or detrimental) influence of alloying effects is transient as a result of homogenization, which may also stop [31] or retard (order-disorder transformation [31], Camagni [74]) the sintering process. It would be highly advantageous to sintering if the vacancy-generating and destroying mechanism could be retained in the system as long as possible. However, this can be done only in some few special cases. (For instance, the diffusion of chromium into the pure $\gamma$-iron grain from alloyed iron powder grains of $\alpha$-structure at the temperature of sintering will cause an $\alpha/\gamma$- transformation,

faulty states induced by the transformation will then persist longer than under the progressing from the contact point between the grains towards the $\gamma$-iron; the influence of a normal alloying effect [40]).

The activation energy and the sintering rate in the assumed range of influence of nickel ($1083^{\circ}$ – $1250^{\circ}$C) cannot be explained on the basis of interdiffusion; one has rather to assume that copper is being eliminated. The increase of the activation energy in comparison with the bulk diffusion of nickel is due to the dissolution of tungsten in nickel (analogous with the 90W. 10Ni mixture).

It is thus exceedingly difficult in multi-component systems to determine in advance the effective diffusion constant of the sintering equation without close investigation, as self-diffusion and interdiffusion and the factors affecting them are not yet fully understood.

### 3.6 The effect of the green density

The rate coefficient k of the sintering equation (equations 6.III and 14.III) can be written

16.III $$k = F(V_o, N)S^n$$

With operation at constant temperature, one finds that the factor $S^n$ is constant (one and the same powder being concerned); consequently the factor affecting the sintering rate is a function of the initial volume and of the contact number.

In the sintering experiments with different green densities (at $1178^{\circ}$C) in each case the impingement exponent i = 2 was obtained, and the sintering equation was thus

17.III $$\alpha / (1 - \alpha) = F(V_o, N)S^n t^n = kt^n = (k_o t)^n$$

At the temperature in question, nickel governs the sintering according to the above reasoning (cf. p. 33). As regards the assessment of the number of contacts, we assume [71] that the contact number drops from six to zero while the fractional porosity increases from unity to $1 - \pi/6$ (cubic packing). In the case under investigation (Table 6), the functions $F(V_o, N)$ and $k_o$, calculated according to equation 17.III, obtain the values given in Table 9, which also contains the experimental $k_o$ values.

Table 9

Calculated $F(V_o, N)$ and $k_o$ and empirical $k_o$ values for various green densities of the specimen

| Green density, $gcm^{-3}$ | 9.25 | 9.83 | 10.33 | 10.70 | 11.15 | 11.77 |
|---|---|---|---|---|---|---|
| Compression, $tncm^{-2}$ | 2 | 3 | 4 | 5 | 6 | 8 |
| $T = 1178^{\circ}C$ | | | | | | |
| $F(V_o, N)$ | 0.65 | 0.73 | 0.83 | 0.91 | 1.02 | 1.19 |
| $k_o$, calc. | 0.51S | 0.61S | 0.75S | 0.86S | 1.03S | 1.31S |
| $k_o$, obs. | 0.120 | 0.115 | 0.117 | 0.125 | 0.123 | 0.115 |
| $t_{17.0}$, h | 58 | 47 | 39 | 34 | 29 | 22 |
| $T = 1320^{\circ}C$ | | | | | | |
| $F(V_o, N)$ | 2.34 | 3.24 | 4.11 | 4.89 | 5.86 | 7.50 |
| $k_o$, calc. | 1.45 | 2.33 | 3.28 | 4.23 | 5.52 | 7.91 |
| $t_{17.0}$, h | 4.7 | 2.4 | 1.4 | 0.9 | 0.6 | 0.3 |

It can be seen from this table that the theoretically calculated $k_o$ value increases more rapidly than the $k_o$ value observed experimentally, which remains almost constant. However, the difference between observed and calculated values cannot be considered large if one takes into account the difficulty of estimating the contact number.

Further, let us compare in the range of influence of tungsten test series a and b (Tables 2 and 3), in which the green densities varied. We assume [71] for the calculation of the contact number of the tungsten grains that a linear relationship exists between the number of contacts and the fractional porosity in the following range: porosity $1 - \pi\sqrt{3}/9$ and contact number 8 (orthorhombic packing), and porosity $1 - \pi\sqrt{2}/6$ and contact number 12 (rhombohedral packing). The number of contacts per tungsten grain is found to be 5.2 in series a and 4.3 in series b. At constant temperature, the following relation between the rate coefficients is valid according to equation 17.III

18.III $$(k_o)_a = (k_o)_b \left[F(V_o, N)_a / F(V_o, N)_b\right]^{1/n}$$

At $1300^{\circ}C$ the a and b series have the rate coefficients $k_{o,a} = 2.6$ and $k_{o,b} = 1.5$ (1/min). From equation 18.III, the rate coefficient of the a series is calculated at $(k_o)_a = 1.53 \cdot (k_o)_b = 2.3$ (1/min), and the agreement with the directly observed value is found to be good.

If the rate coefficient at 1321°C is calculated according to equations 14.III and 17.III ($\gamma_W$ = 4000 ergs per $cm^2$, R = $10^{-4}$ cm, N = 5.2, $D_W$ = $1.5 \cdot 10^{-11}$ $cm^2/s$), it is found to have the value (in series a) of $k_o$ = 0.31 (1/min). On comparing this with the observed value (Table 2) $k_o$ = 4.8 (1/min), it can be noted that the calculated value is about one tenth of this. According to the equations, the grain size affects the rate coefficient by a factor of $R^{-3}$; reduction of the grain size to half of what it was assumed to be is sufficient to increase the calculated rate coefficient so that agreement with the observed value is achieved. When one considers the irregular shape and the porous structure of the tungsten grains, and their grain size distribution, one is justified in attributing the difference between calculated and observed rate coefficient to the difficulty of determining the effective grain size and the number of contacts.

The $k_o$ and $F(V_o, N)$ values computed for different green densities from equation 18.III, employing the above-mentioned assumption as regards the number of contacts and the observed rate coefficient (at 1321°C), are compiled in Table 9. In this case, the number of contacts has already a marked effect upon the rate coefficient.

Although the effect of the green density of the specimen upon the rate coefficient is not very remarkable (in temperature range C), it has a considerable influence upon the rate of decrease in volume of the specimen, or (by definition) upon the sintering rate.

According to equation 17.III, the rate of change of the porous volume fraction ($\alpha$) has the form

$$19.III \qquad d\alpha/dt = n(1-\alpha)^2 k t^{n-1} = n(1-\alpha)^2 \left[\alpha/(1-\alpha)\right]^{1-1/n} k^{1/n}$$

Fig. 12A shows the rate of change as a function of the $\alpha$ fraction at 1178°C. As in this test series the rate coefficient (k) was approximately constant, the rate of transformation $d\alpha/dt$ is also in this instance independent of the green volume (the specific density $1/\varrho_o$ may be used instead of the green volume).

The rate of decrease in volume of the specimen, i.e. its sintering rate, has the form $-dV_s/dt = (V_o - V_{te})\, d\alpha/dt$, according to equation 7.III. This equation implies that the sintering rate rises with increasing green volume, which is indeed a fact generally known but little investigated [24, 26]. Figs. 20A and 20B show the sintering rate and the volume of the specimen as functions of the $\alpha$ fraction.

From the viewpoint of the ultimate result of sintering, an important characteristic is the rate of change in volume at a given fraction of the theoretical volume, i.e. at a given value of relative density (cf. under 3.8). Let us consider the sintering rate for $V_s = v$, $V_o \gg v > V_{te}$. The sintering rate has the form (equation 8.III):

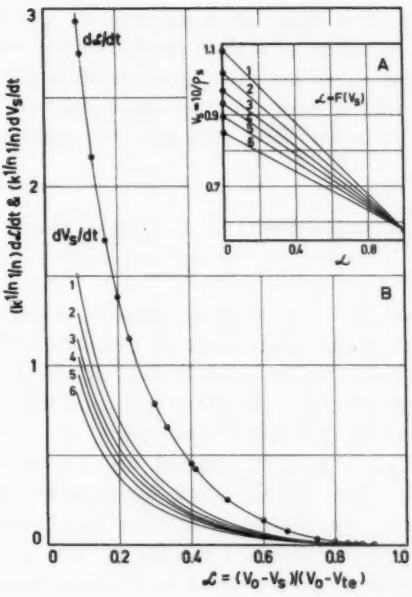


Fig. 20 Rate of sintering as a function of the pore fraction.

20.III $$dV_s/dt = \text{const.} / ((V_o/V_{te}) - 1)\,((V_o/V_{te}) - (v/V_{te}))^m$$

where $m = (1/n) - 1$. Since 1 $n>0$, $m>0$.

The equation reveals that the sintering rate at a given fraction (v) of the ultimate volume becomes less with increasing green volume. In the general case, where the number of contacts changes more strongly with changing green volume, the same observation applies, as the function $F(V_o, N)$ decreases with increasing green volume.

In view of the economy of sintering, it is important that the specimens have a high green density. Unless this condition is satisfied, long and expensive treatment in the furnace is required to give them an adequate ultimate density.

The sintering time required to attain the density 17.0 g/cm$^3$ (98.4 %) at 1178$^o$C is shown in Table 9. Since at this temperature tungsten cannot yet participate in the sintering process, it is hardly possible to achieve full density,

even with a long treatment time. (It is true that the dissolution and precipitation of tungsten by mediation of a bond phase may have a favourable effect if there is sufficient time.) For the same green densities the times corresponding to a temperature of 1321°C have also been calculated, and entered in Table 9. They are in agreement on the whole with practical experience.

### 3.7 The sintering equation in the light of the results reported in publications

Study of the suitability of our sintering equation (equations 10.III to 11.III) in comparison with empirical values stated in publications is greatly impeded by the lack of the associated data required in such considerations. As, moreover, such results have to be read from diagrams, it is generally only possible to make qualitative observations on the basis of such values.

Clark and White [13] have investigated the mechanism of sintering with spherical and angular copper grains. Their experimental results are reproduced in Figs. 21 and 22. The results relating to the change of relative density ($\varrho_s / \varrho_{te}$) in the powder compact as a function of time, obtained with spherical grains, is seen in Fig. 21A. As is revealed in Fig. 21B, the results show very close agreement with sintering equation 11.III (impingement exponent i = 2). The sintering equations for different temperatures are (time stated in hours):

$$1020^{\circ}C \quad \alpha / (1 - \alpha) = (4.9 \cdot 10^{-2} t)^{0.58}$$

$$925^{\circ}C \quad \alpha / (1 - \alpha) = (1.1 \cdot 10^{-2} t)^{0.58}$$

If calculation is made according to the model of Kingery and Berg [8] (values for calculation in [8]), one obtains the following values for the rate coefficients: $1020^{\circ}C/k_o = 3.7 \cdot 10^{-2}\ h^{-1}$, and $925^{\circ}C/k_o = 0.7 \cdot 10^{-2}\ h^{-1}$. The calculated and observed results show excellent agreement. From experimental results, the activation energy for the sintering of spherical bodies is found to be 48 kcal/mol. This is not markedly different from the activation energy of self-diffusion of copper employed in the calculations, 54 kcal/mol.

Figs. 22A and 22B show the results obtained on sintering angular copper grains. They display close agreement with the sintering equation. The equations found by evaluating the straight lines are of the form:

$$1020^{\circ}C \quad \alpha / (1 - \alpha) = (6.2 \cdot 10^{-1} t)^{0.64}$$

$$925^{\circ}C \quad \alpha / (1 - \alpha) = (1.4 \cdot 10^{-1} t)^{0.64}$$

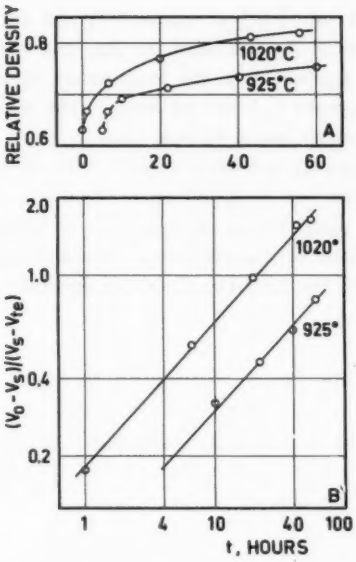


Fig. 21 Shrinkage isotherms, spherical grain.

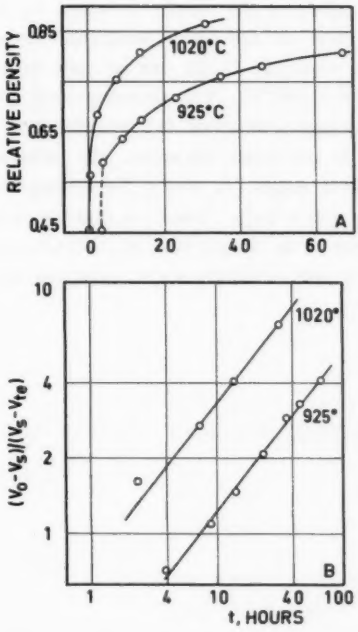


Fig. 22 Shrinkage isotherms, angular grain.

The rate coefficients calculated on the basis of the ideal model [8] are: $1020^{o}C/k_{o} = 1.5 \cdot 10^{-2}\ h^{-1}$ and $925^{o}C/k_{o} = 3.0 \cdot 10^{-3}\ h^{-1}$. Comparison of the results shows that, in the packing of angular grains, the rate coefficients are about 40 to 50 times those in the packing of spheres, the basis of the calculations. For the activation energy, the value 53 kcal/mol is obtained, and evidently the sintering mechanism has not changed. As both powders have approximately the same time exponent, the impingement exponent also can be assumed to be close to the correct value. The great difference as regards rate coefficient may be due to the increased number of contacts, or even rather to the fact that the mean grain size is not given in the investigation cited.

The equation of the form 11.III is also in close agreement with the investigation of Rhines [17] relating to copper powder. This powder was sintered in hydrogen at $800^{o}$, $900^{o}$ and $1000^{o}C$. The time of treatment varied between 1 and 1000 hours. For the time exponent, the value 0.3 is obtained when the impingement exponent is taken as i = 2, and the activation energy is found to be about 82 kcal/mol.

Study of the results obtained by Duwez et al. [26] is impeded by the lack of data on the green densities. On the basis of the available results, however, the equation 11.III can be said to be well applicable in the temperature range $760^{\circ}$ — $982^{\circ}$C. The sintering time varied between 0.5 and 64 hours. The time exponent was about 0.2 and the activation energy about 96 kcal/mol.

In numerous instances, the process of sintering has been studied only in its initial stages, in which the impingement factor has little influence (Okamura et al. [22 — 24]). There is thus no reason to study results of this type, of which there is an ample choice, because on the basis of our preceding considerations they will certainly show close conformity with the sintering equations derived.

# IV DISCUSSION OF THE PROPERTIES OF THE SINTERED SPECIMENS

## 1. X-RAY DIFFRACTION STUDY

The test specimen sintered of 90W.10(2Ni.Cu) powder mixture has the structure of a packing of fairly round tungsten grains, whose interstices are occupied by a binder phase consisting of copper, nickel and tungsten. X-ray studies were carried out in an attempt to determine the structure of the tungsten grains, the quantity of tungsten dissolved in the binder phase, and the processes of transformation that may occur in the binder phase.

### 1.1 The structure of the tungsten grains

A number of specimens were sintered for purposes of measurement, varying sintering times (0.25 to 11 hours) and sintering temperatures ($1000^{\circ}$ ... $1400^{\circ}$C) being applied and the specimens being quenched in water (with 5 % NaCl added). A powder sample was taken, with a file, from the centre of the cylinder after it had been sawn in two longitudinally; the powder was annealed for 2 ... 3 minutes at $1000^{\circ}$C in a vacuum in order to relieve the working stresses. For comparison, a sample of the original tungsten powder was also subjected to the same measurements. Radiation from a copper x-ray tube was employed.

The measurements resulted in one and the same lattice constant for all samples (at $20^{\circ}$C), namely, $a = 3.1593 \pm 3$ kx.

In publications, it is stated that tungsten has a lattice constant (at $20^{\circ}$C) of $a = 3.1586$ kx [41]. According to the results of various investigators, error lim-

its of ± 0.0003 kx can be assigned to this value. In the present investigation, the value found is thus slightly in excess of this. Price et al. [59] state that the tungsten grains in a specimen sintered from 93W.7(2.5Ni.Cu) powder mixture are single crystals, and on chemical analysis prove to consist of pure tungsten. Despite the small differences in lattice constant, it can be assumed that in the present case the tungsten grains are still pure after sintering. It is true that the influence of small nickel quantities upon the lattice constant of tungsten is unknown, but the mixture employed in this instance differs to a sufficiently small extent from Price's mixture to justify the contention that its behaviour is similar.

## 1.2 The structure of the binder phase

The composition of the binder phase was determined by comparison between the lattice constants of specimens quenched from various temperatures and of standard samples containing varying quantities of tungsten. The standard samples were prepared by melting or sintering 2Ni.Cu mixture, with the admixture of varying quantities (0 to 20 %) of tungsten powder. Suitable pieces were cut from the samples, enclosed in evacuated quartz ampoules, melted and quenched in salt water. The working stresses of the powder sample were relieved by annealing for 2 ··· 3 minutes at 1000°C. The lattice constants of the standard samples were determined with the aid of radiation supplied by Cu and Co tubes (with the Co tube radiation lines obtained at very large angles in the initial part of the test series).

The measurements showed that the atomic percentages of the tungsten in solution in the standard samples had a linear relationship with the corresponding lattice constants. The straight line had the equation

$$1.IV \qquad a_x(kx) = 3.5442 + 3.83 \cdot 10^{-3} X \,,$$

where X is the atomic percentage of the tungsten in solution. The deviation of the measured values amounted to about $3 \cdot 10^{-4}$ kx only. The value 3.5442 ± 3 kx was found for the lattice constant of the 2Ni.Cu alloy, and this fits in between the values interpolated from published reports [41], a = 3.5446 kx (Owen et al.) and a = 3.5419 kx (Coles).

As, in relation to the binder phase in the specimens sintered from 90W.10 (2Ni.Cu) powder mixture, the measurements were impeded by the strong absorption of tungsten, they were carried out with a mixture containing only 50 % of tungsten. The result of the binder phase analysis is shown in Table 10. The lattice constant value for the last temperature in the table (1409°C) is not of the

Table 10
Lattice constants of the binder phase

| T °C | $a_o$ kx | W at. wt % | W wt % |
|---|---|---|---|
| 1215 | 3.5693 | 6.56 | 17.7 |
| 1259 | 3.5703 | 6.80 | 18.2 |
| 1296 | 3.5712 | 7.04 | 18.8 |
| 1348 | 3.5729 | 7,48 | 19.8 |
| 1409 | (3.5770) | (8.56) | (22) |

same degree of accuracy as the others. This specimen partially melted, and the film shows broad, doubled diffraction lines (inhomogeneity, under cooling; Vogel [75]).

Comparison of the result obtained with the Ni-W phase diagram [76] reveals that the change in $\alpha$ solid solubility is similar to this result. Obviously, copper causes only reduction of the solubility of tungsten (Ni-W: 39 % W at 1495°C). Price et al. [59] report, for the 93W.7(2.5Ni.Cu) mixture, the tungsten solubility of the binder phase at 17 % (temperature probably 1421°C), a value that appears too low.

Taking the tungsten solubility at 18.8 % (1296°C), then a density of 9.982 g/cm$^3$ and a content of 12.32 % for the binder phase was calculated. The theoretical density of the heavy alloy under investigation will then be 17.282 g/cm$^3$.

### 1.3 Transformation phenomena in the binder phase

As the binder phase under investigation closely resembles the Ni-W-system, an investigation was made of the occurrence of the corresponding intermetallic compounds in it. The b. c-tetragonal $Ni_4W$ compound in the Ni-W-system is formed below 970° ± 10°C. In order to study the influence of copper, several Ni-W-Cu powder mixtures were prepared. The powder mixtures had the compositions 45W.55Ni, 45W.55(10Ni.Cu), 45W.55(5Ni.Cu) and 45W.55(2Ni.Cu). These mixtures were sintered for about 12 hours at 1305°C, heat-treated at 900°C for 30 hours, and subsequently investigated by means of x-rays. The samples without copper yielded the $Ni_4W$ lines reported by Epremian and Harker [77]. The same result was obtained for the sample corresponding to the composition (10Ni.Cu). With the (5Ni.Cu) mixture, weak lines could still be noted which were not accountable to Monel or tungsten. In the sample corresponding to the 2Ni.Cu ratio employed in the sintering investigation, no further foreign lines could be ob-

served and it is therefore probable that copper inhibits the formation of at least a permanent $Ni_4W$ compaund (at 900°C).

The 90W. 10(2Ni. Cu) mixture shows considerably different mechanical properties, dependent upon whether the specimen is quenched from the sintering temperature, or slowly cooled. Since on the basis of this investigation no signs could be noted of the precipitation of any stable foreign phase, it is likely that the impairment of the characteristics is due to precipitation of tungsten on the grain boundaries during slow cooling. According to our studies, the solubility of tungsten in the binder phase (below 1400°C) was dependent upon temperature to only a slight extent. However, since the binder phase takes the form of thin films surrounding the tungsten grains, even small precipitated quantities may produce noteworthy changes in the mechanical properties.

## 2. THE PHYSICAL CHARACTERISTICS OF THE SINTERED SPECIMEN

Tensile test bars, with a green density of about 10.3 $g/cm^3$, were prepared for the study of the electrical conductivity, the damping and the mechanical properties of the product sintered from the 90W. 10(2Ni. Cu) powder mixture.

For sintering, the bars were placed in a boat of iron, lightly packed in aluminium oxide. Sintering was effected by quickly pushing the boat with an iron rod into the hottest zone of the furnace, and, after sintering, rapidly again into the cooling zone (water cooling). The temperature of the large molybdenum furnace (Surahammars Bruks Aktiebolag, Sweden) employed for the sintering was optically controlled. The temperature in the interior of the boat was measured potentiometrically by means of a platinum vs. platinum + 13 % rhodium thermocouple.

### 2.1 Shrinkage of the tensile test bars

The density of the sintered tensile test bars, as a function of time and temperature, can be seen in Fig. 23. At low temperatures, the shrinkage of the bars obeyed the equation 10.III. The time exponent varied between 0.71 and 0.74 (i = 2), and was thus slightly higher than that for the cylinder specimens (Tables 2 and 3). This may be due to the fact that the change was not the same in all directions. The rate coefficients $k_o$ were approximately the same as for the cylinder specimens. However, they displayed greater deviation at different temperatures, because the sintering (on an industrial scale) was not so well controlled as in the laboratory measurements.

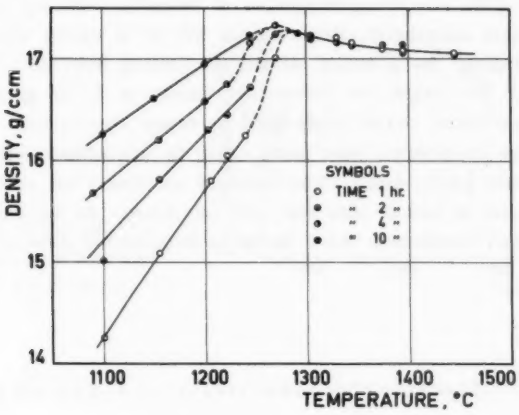


Fig. 23 Density of the tensile test bars as a function of time and temperature.

At high temperatures, the density is seen to decrease from the theoretical value, which is attained within a temperature range of about 1250° ··· 1320°C, dependent upon the sintering time and the compression.

The volume fraction of the binder phase in the dense product is 21 %. The porosity of the densest regular packing of spheres is 26 % (rhombohedral packing [71]). As the tungsten grains in the sintered specimens are inclined towards roundness, it is necessary to assume self-sieving of the fine grain classes into the interstices of the large grains for the theoretical density of packing to be achieved. When theoretical density has been rapidly attained at high temperatures, the equilibrium between the grains begins to establish itself. The fine tungsten grain classes are dissolved in the binder phase, which becomes saturated. Since a small grain is in equilibrium with a solution of higher concentration than a large grain, the consequence is discharge of the supersaturation of the solution on to the surface of a large grain, and thus a strong growth of grains. As a result of this grain growth, small grains disappear, the grain sizes become more equalized, and a uniform framework of rounded tungsten grains in mutual contact is formed. When the product cools down from a high temperature (equilibrium structure), the tungsten frame shrinks much less than the binder phase (the difference in thermal expansion is about two- to threefold). This produces strong compressive stress in the framework and tensile stress in the binder phase. The stresses result in detachment of the binder phase from the framework (cf. Baxter [52]), as the tungsten grains cannot follow the change of the binder phase, because with the equal-

ization of their grain size the prerequisites of theoretical density have been lost. If one assumes that the tungsten frame shrinks only to an extent which corresponds to thermal expansion, the ultimate density on cooling from 1300°C is found to be 17.06 g/cm$^3$ (as against the theoretical density of 17.28 g/cm$^3$), which is approximately equivalent to the result found by actual observations. (The thermal expansions of the components have been taken in accordance with Apblett and Pellini [78], Esser [41], etc.). The decrease in density on cooling from still higher temperatures is greater than that just calculated. As the melting contraction of Monel (+W) is unknown, there can be no discussion of these temperatures.

## 2.2 Electrical conductivity and damping

The results of the conductivity measurements with the tensile test bars, as a function of sintering temperature, are shown in Fig. 24. Their conductivity increases with time and temperature, a change consequent upon the growth of contact areas between the grains [5]. The change of conductivity with density for the tensile test bars and cylinder specimens (Sigma-test) is to be seen in Figs. 25A and 25B. The relationship is approximately linear (below 1300°C) and independent of sintering time and temperature (analogous results: Duffield [79], Grootenhuis [80], etc.).

It can be seen from the figures that, beyond a temperature of about 1320°C, the conductivity begins to decrease with increasing temperature. A decrease in conductivity and in density begins in the same temperature range, and it is thus also probable that the same causes are responsible for both. The cracking of the binder phase and its peeling from the tungsten grains raises the contact resistances. This, together with internal stresses, results in impaired conductivity. Above the said temperature, strong grain growth also takes place, which reduces the conductivity [79]. This is reflected, for instance, in the effect of time upon conductivity at high temperatures.

Homogeneous (2Ni. Cu) alloy has the conductivity $\varkappa = 21.4 \cdot 10^6$ $(1/\Omega m)$ [81]. If one employs the volume mixing rule, one finds for the conductivity of the investigated mixture $\varkappa = 18.8 \cdot 10^6$ $(1/\Omega m)$. The conductivity corresponding to the dense product is, according to direct measurement, about $\varkappa = 13 \cdot 10^6$ $(1/\Omega m)$.

The change of damping with time and temperature is shown in Fig. 26 (The plots represent the inverse, relative). The Q value closely follows the change in conductivity in the entire range of temperature; as it is highly structure-sensitive property, it serves to strengthen the idea of structural changes brought about by stresses in the specimens cooled from high temperatures.

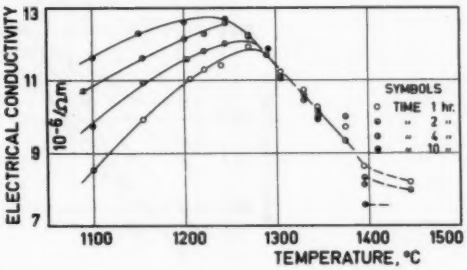


Fig. 24 Conductivity of the tensile test bars as a function of time and temperature.

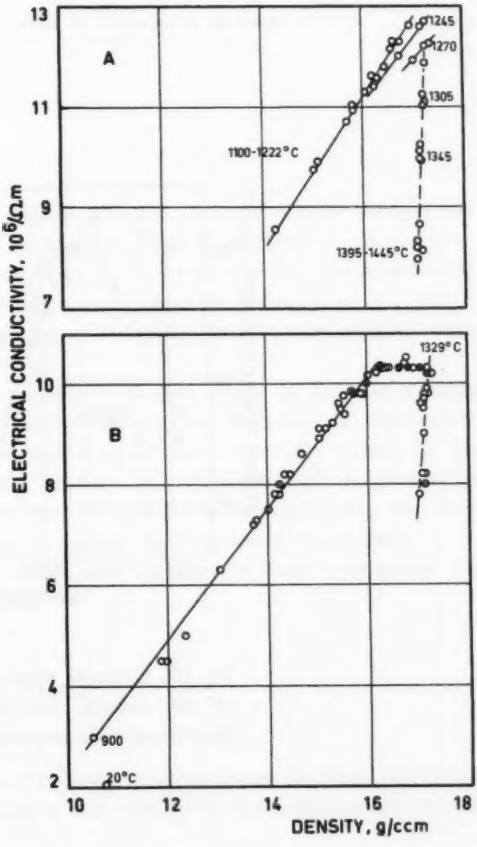


Fig. 25 Conductivity of the tensile test bars and cylinders as a function of density.

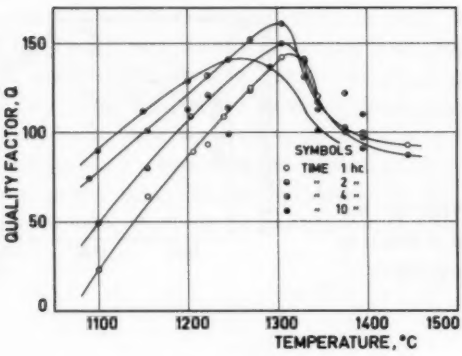


Fig. 26 Quality factor Q of the tensile test bars as a function of time and temperature.

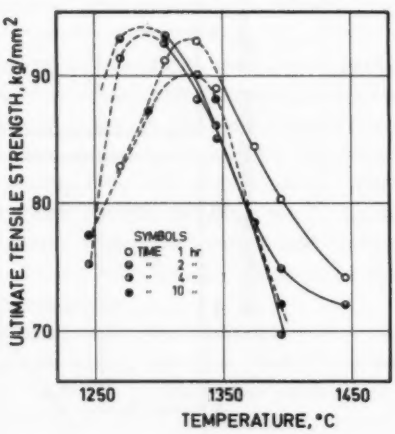


Fig. 27 Ultimate tensile strength of the tensile test bars as a function of time and temperature.

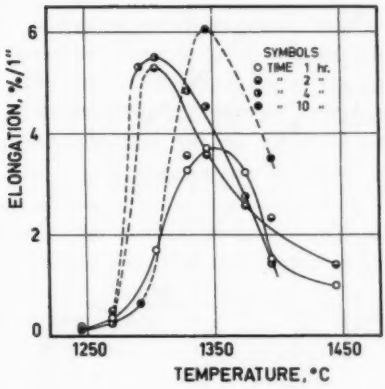


Fig. 28 Elongation of the tensile test bars as a function of time and temperature.

## 2.3 Mechanical properties

The results of measurement concerned with the ultimate tensile strength and elongation of the tensile test bars are shown in Figs. 27 and 28.

At the beginning of sintering, the mechanical strength is directly proportional to the growing contact surface between the grains (Bockstiegel et al. [21]). Consequently the mechanical properties of the alloy investigated improve when the density of the test bars is increased.

According to Fig. 27, the ultimate tensile strength begins to decrease abruptly beyond the temperature interval $1300^{o} \pm 25^{o}C$. The decrease in mechanical strength of the product sintered at high temperatures is probably caused by the same factors as that relating to the density. In consequence of the present results, the ultimate tensile strength and the elongation obviously obey the same laws in their changes, which serves to support the conception stated above.

The grain size determined for the tensile test bars at high temperature (by planar analysis) obeyed the equation

$$D = kt^{n}, \qquad 2.IV$$

where D is the grain diameter (in $10^{-4}$ cm), t is the time, in hours, and n and k are constants. The time exponent n was constant at the temperatures investi-

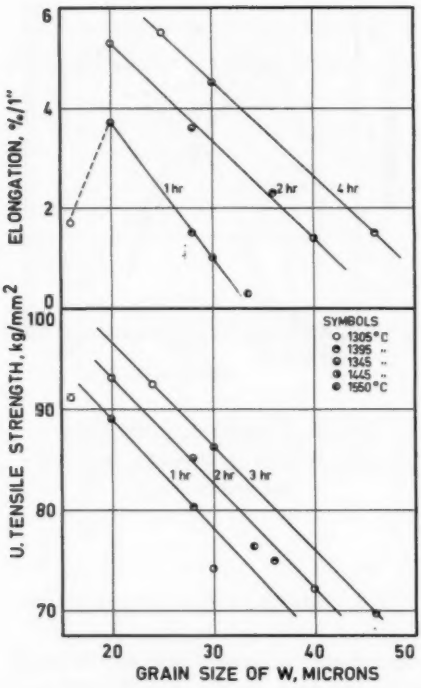


Fig. 29 Elongation and ultimate tensile strength of the tensile test bars as a function of grain size.

gated (as a rule temperature exerts an influence [82]) and had the magnitude 0.30 ± 0.03. The constant k was a function of temperature (the values at 1305°, 1345°, 1395°, 1445°, and 1550°C were respectively 16.0, 20.0, 29.4, 30.0 and 34.0. From its change, the activation energy at temperatures below 1400°C is found to be about 120 kcal/mol, and above 1400°C about 20 kcal/mol. (The values show considerable deviation.) The grain growth in the mixture under investigation thus does not seem to differ from the growth mechanism of dense substance, as no pore size and pore volume modification was necessary, as is usual in the growth equations of sintered bodies (Hausner [82], etc.). When one considers that the activation energy (below 1400°C) is very high, there is added weight given to the assumption that the solid state in the binder phase is retained through the influence of the dissolution of tungsten, despite the low melting point

of the (2Ni.Cu) alloy. At high temperatures (above 1400°C), the grain size readily increases because the binder phase is in the molten state.

Comparison of the grain size and the mechanical properties provides the result shown in Fig. 29. It can be seen that the mechanical properties are certainly impaired with increasing grain size, but that the effect of grain size upon them is, as compared with the influence of temperature, negligibly small, particularly below 1400°C.

As regards its structure, the mixture under investigation resembles a number of cermet and hard metal systems. The mechanical properties of the latter are primarily dependent upon the quantity of binding agent and upon grain size. If there is too little of the binder phase (e.g. Co, Ni, Al, etc.), the highest possible strength will not be attained. If there is sufficient of it, or more than is needed, a maximum of mechanical strength will be obtained at a certain grain size (Gurland et al. [83]). The best mechanical strength is then also related to the least mean free path between the grains (soldering effect: e.g. Stefans theory [84]). Optimum strength is obtained in hard metal and cermet systems (usually dependent upon on grain size, but not on grain shape) if the binder phase amounts to 25 ··· 30 per cent by volume, corresponding to the pore volume of the densest packing of spheres (e.g. Co+WC, Gurland [83]; TiC+Co, MgO+Co, etc., Harris [85]).

In the investigated mixture, with its rounded tungsten grains, the binder phase can be assumed as having the greatest significance on the basis of what has been said above. As the binder phase amounts to only 21 per cent. by volume, it is likely that even from the beginning the mechanical properties are such that it is difficult to alter them without changing the proportions of the phases.

## SUMMARY

1. A study has been made of the phenomena which occur when a powder mixture of 90W. 10(2Ni. Cu) type, belonging to the range of heavy metal alloys, is sintered at high temperatures.

2. The shrinkage of the powder specimens was studied with the aid of an optical dilatometer developed for this purpose; this made possible the elimination of the commonest errors (green density variation, heating time, etc.) in the direct measurement frequently employed in powder investigations.

3. On the basis of accurate shrinkage observations, it could be noted that the sintering obeyed a new sintering equation, which is valid in the entire sintering range for pure substance systems as well as for the investigated multi-component systems.

4. An attempt has been made also to give an analytical interpretation of the new sintering equation on the basis of the diffusion theory of ideal models. As the ideal models have a strictly limited range of validity, there was introduced in the treatment of sintering the concept of what is termed the impingement factor as used frequently in the treatment of precipitation, and growth and decomposition transformations occurring in the solid state of metals, but not, as far as is known in connection with sintering processes.

5. The new analytical representation of the sintering process is in close agreement with existing theory, as well as with empirical observations.

6. Furthermore, the sintering of heavy metals obeys the new time law. On the basis of the observations, it can be noted that their manufacture in a solid state is technically and economically advantageous; such manufacture can without special arrangements then be linked to the normal processing procedure of a powder-processing factory. It can be said, on the basis of the behaviour of heavy alloy metal, that the earlier method used in its manufacture, "liquid phase sintering"

at high temperature constitutes "oversintering", and thus, in the present instance, is expensive and otherwise not to be recommended in view of its generally accompaniment of impairment of the properties of the product.

## REFERENCES


1. P. Schwarzkopf, Powder Metallurgy Bulletin, 1948, 3, 74; 1950, 5, 5.

2. W. E. Kingston, The Physics of Powdermetallurgy, New York, 1951, 1.

3. A. Smekal, Powder Metallurgy Bulletin, 1949, 4, 120, ref. 2., 27.

4. A. J. Shaler, Met. Trans., 1949, 185, 796.
   A. J. Shaler, J. Wulff, Ind. Eng. Chem. 1948, 40, 838.
   A. W. Postlethwaite, A. J. Shaler, ref. 2., 189.

5. G. C. Kuczynski, Met. Trans., 1949, 185, 169.
   J. Appl. Phys., 1950, 21, 632, 1339; 1949, 20, 1160.
   Acta Met., 1956, 4, 58, ref. 2., 202.

6. N. Cabrera, Trans. AIME, 1950, 188, 667.

7. P. Schwed, Trans. AIME, 1950, 191, 245.

8. D. W. Kingery, M. Berg, J. Appl. Phys., 1955, 26, 1205.

9. C. Herring, J. Appl. Phys., 1950, 21, 301.

10. R. L. Coble, J. Am. Ceram. Soc., 1958, 41, 55.

11. J. Frenkel, J. Techn. Phys. (USSR), 1945, 9, 385.

12. J. K. Mackenzie, R. Shuttleworth, Proc. Phys. Soc., 1949, 62B, 833.

13. P. W. Clark, J. White, Trans. Brit. Ceram. Soc., 1950, 49, 305.
P. W. Clark, H. J. Cannon, J. White, Trans. Brit. Ceram. Soc., 1953, 52, 1.

14. A. D. Smigelskas, E. O. Kirkendall, Trans. AIME, 1947, 171, 130.

15. L. C. C. da Sylva, R. F. Mehl, J. Metals, 1951, 3, 155.

16. F. R. N. Nabarro, Solids Symposium, Bristol, 1948, 75, 99, ref. 13.

17. F. N. Rhines, C. E. Birchenall, L. A. Hughes, Trans. AIME, 1950, 188, 378.

18. B. H. Alexander, R. W. Balluffi, J. Metals, 1950, 2, 1219, Acta Met., 1957, 5, 666.

19. R. W. Balluffi, L. L. Seigle, Acta Met., 1955, 3, 170.

20. J. E. Burke, J. Am. Ceram. Soc., 1957, 40, 80.

21. G. Bockstiegel, Trans. AIME, 1956, 206, 580.
G. Bockstiegel, G. Masing, G. Zapf, Appl. Sci. Res., 1945, A4, 284.

22. T. Okamura, S. Kikuta, Y. Masuda, Sci. Rep. RITU, 1949, A1, 357.

23. Y. Masuda, S. Kikuta, Sci. Rep. RITU, 1951, A3, 435.

24. A. Takasaki, Sci. Rep. RITU, 1951, A3, 1; 1953, A5, 477.

25. G. Cizeron, P. Lacombe, Rev. de Met., 1955, 52, 771; 1956, 53, 818.

26. P. Duwez, H. E. Martens, Trans. AIME, 1949, 185, 571.
C. B. Jordan, P. Duwez, Trans. AIME, 1949, 185, 96.

27. H. H. Hausner, Pulvermetallurgie, I Plansee Seminar, 1953, 146.

28. J. R. Dunning, B. R. Drentice, Advances in Nuclear Engineering II, New York, 1957, 209.

29. E. Raub, W. Plate, Z. Metallkde, 1949, 40, 206.

30. E. M. Onitsch-Modl, Planseeberichte für Pulvermetallurgie, 1955, 3, 42. Planseeproceedings, 1955, 427.

31. P. Duwez, Powder Metallurgy Bulletin, 1949, 4, 143, 167.
P. Duwez, C. B. Jordan, Trans. ASM., 1949, 41, 194, ref. 2., 230.
P. D. Howat, R. L. Craik, J. P. Cransten, J. Inst. Met., 1951 – 52, 80, 353.

32. S. Weinbaum, J. Appl. Phys., 1948, 19, 897.

33. K. Torkar, H. Götz, Z. Metallkde, 1955, 46, 371.
K. Torkar, H. Mariacher, Planseeberichte für Pulvermetallurgie, 1955, 3, 78.

34. W. Köster, J. Raffelsieper, Z. Metallkde, 1951, 42, 387; 1952, 43, 37.
H. Staude, Physikalisch-Chemisches Taschenbuch II, Leipzig, 1949, 1666.

35. F. W. Glaser, Met. Trans., 1949, 185, 475. Powder Metallurgy Bulletin, 1949, 4, 19.

36. J. M. Butler, T. P. Hoar, J. Inst. Met., 1951 – 52, 80, 207.

37. F. Thümmler, Planseeberichte für Pulvermetallurgie, 1958, 6, 2.

38. J. T. Jones, P. K. Maitra, I. B. Cutler, J. Am. Ceram. Soc. 1958, 41, 353.
G. K. Layden, M. C. Mc Quarrie, J. Am. Ceram. Soc., 1959, 42, 89.

39. F.-R. Meyer, Grete Ronge, Angew. Chemie, 1939, 52, 637.

40. S. Mäkipirtti, Lic. Thesis, The Institute of Technology (Helsinki), 1958, 17.

41. W. B. Pearson, A Handbook of Lattice Spacings and Structures of Metals and Alloys, London 1958, 627, 631, 884, 592.

42. H. S. Peiser, H. P. Rooksby, A. J. C. Wilson, X-ray Diffraction by Polycrystalline Materials, London 1955, 392, 366.

43. H. Schreiner, G. Glawitsch, Z. Metallkde, 1954, 45, 102.
H. Schreiner, Pulvermetallurgie, I Plansee Seminar, 1953, 203.

44. W. Seith, A. Kottmann, Angew. Chemie, 1952, 64, 379.
W. Seith, K. Budde, Aus Forschung und Produktion (Degussa), 1953, 87.

45. H. Bückle, Pulvermetallurgie, I Plansee Seminar, 1953, 77.

46. W. Seith, Diffusion in Metallen, Berlin 1955, 105, 52, 53, 61, 108.

47. G.-M. Schwab, Handbuch der Katalyse, Bd. 6., Wien 1943, 420.
G.F.Hüttig, K. Addlassning, O. Foglar, ref. 2., 180.

48. K. Hauffe, Reaktionen in und an Festen Stoffen, Berlin 1955, 358, 383.

49. R. E. Hoffmann, F. W. Pikus, R. A. Ward, J. Metals, 1956, 483.

50. R. A. Swalin, A. Martin, J. Metals, 1956, 567.
R. A. Swalin, A. Martin, A. Olson, Am. Inst. Mining. Met. Petrol Engrs., 1957. 209, 936.

51. N. M. Parikh, M. Humenik, J. Am. Ceram. Soc., 1957, 40, 315.
A. Bondi, Chem. Review, 1953, 52, 2.

52. J. R. Baxter, A. L. Roberts, Iron Steel Inst., London Symposium Group II, 1954, 63, 70.

53. H. J. Boos, Planseeberichte für Pulvermetallurgie, 1958, 6, 17.

54. P. L. Gruzin, Dokl. Akad. Nauk. (SSSR), 1955, 100, 65, 67.

55. R. E. Hoffmann, D. Turnbull, J. Appl. Phys., 1952, 23, 1409.
R. E. Hoffmann, D. Turnbull, E. W. Hart, Acta Met., 1955, 3, 417; 1957, 5, 74.

56. R. Lindner, Sec. UNC of Atomic Energy, 1958, A/Conf. 15/P/167.

57, E. Nachtigall, Plansee Proceedings, 1955, 313.

58. V. P. Wasiljev, Zavodskaja Laboratorija, 1956, 6, 689.

59. G. H. S. Price, C. J. Smithells, S. V. Williams, J. Inst. Met., 1938, 5, 117.
G. H. S. Price, S. V. Williams, C. J. O. Garrard, G.E.C. Journal, 1941, 11, 223.

60. H. S. Cannon, F. V. Lenel, Pulvermetallurgie, I Plansee Seminar, 1953, 106, F. V. Lenel, ref. 2., 238.

61. D.T. Livey, P. Murray, Plansee Proceedings, 1955, 375.

62. E.C. Green, D.J. Jones, W.R. Pitkin, Iron Steel Inst., London Symposium, Group IV, 1954, 1.

63. W.D. Jones, Acta Met., 1959, 7, 223.

64. M. Avrami, J. Chem. Phys., 1940, 8, 212.

65. W.A. Johnson, R.F. Mehl, Trans. AIME, 1939, 135, 416.

66. B.S. Lement, M. Cohen, Acta Met., 1956, 4, 469.

67. J.B. Austin, R.L. Ricket, Trans. AIME, 1939, 135, 396.

68. M. Hickley, J.H. Woodhead, J. Iron Steel Inst., 1954, 176, 129.

69. W.E. Garner, Chemistry of the Solid State, London 1955, 207.

70. J.F. Quirk, J. Am. Ceram. Soc., 1959, 42, 178.

71. J.M. Dalla Valle, Micromeritics, New York 1948, 128.

72. J.B. Darby, C.T. Tomizuka, R.W. Balluffi, J. Appl. Phys., 1959, 30, 104.

73. N.H. Nachtrieb, Sec. UNC of atomic Energy, 1958, A/Conf.15/P/718.

74. P. Camagni, Sec. UNC of Atomic Energy, 1958, A/Conf. 15/P/1365.

75. M. Hansen, Der Aufbau der Zweistofflegierungen, Berlin 1936, 961.

76. Metals Handbook, ASM, Ohio 1948, 1235.

77. E. Epremian, D. Harker, Met. Trans., 1949, 185, 267.

78. W.R. Apblett, W.S. Pellini, ASM Preprint no. 2W, 1952, 13.

79. A. Duffield, P. Grootenhuis, J. Inst. Met., 1958 – 59, 87, 35.

80. P. Grootenhuis, R.W. Powell, R.P. Tye, Proc. Phys. Soc. 1952, B65, 502.

81. The Nickel Bulletin, 1952, 25, 226.

82. W. Smoluchowski, Imperfections in Nearly Perfect Crystals, 1952, 459. (Pocono Manor Symposium)

83. J. Gurland, P. Bardzil, J. Metals, 1955, 311.

84. J. J. Bikerman, Surface Chemistry, New York 1948, 126, 358.

85. G. T. Harris, H. C. Child, Iron Steel Inst., London Symposium, Group IV, 1954, 30, 73.

# THE LAST VOLUMES OF ACTA POLYTECHNICA

## *Chemistry including Metallurgy Series*

(The predecessor of Acta Polytechnica Scandinavica)

### Volume 3

**Nr 6** CHRISTIANSSON, B: *Studies on Low-temperature Carbonisation of Peat and Peat Constituents.* Acta P 124 (1953), 128 pp, Sw. Kr 16: 00 UDC 662.731

**Nr 7** NÖMMIK, H: *Fluorine in Swedish Agricultural Products, Soil and Drinking Water.* Acta P. 127 (1953), 121 pp, Sw. Kr 16: 00 UDC 545.83:546.16 553.634.1(485)

**Nr 8** ALLANDER, C G: *Untersuchung des Adsorptionsvorganges in Adsorbentenschichten mit linearer Adsorptionsisotherme.* Acta P 130 (1953), 160 pp, Sw. Kr 10: 00 UDC 541.183.57

**Nr 9** BRAAE, B: *The production of Transformer Oil by Hydrogenation of Swedish Shale Oil.* Acta P 136 (1954), II + 76 pp, Sw. Kr 12: 00 UDC 665.452.2:66.094.14

### Volume 4

**Nr 1** SJÖSTRÖM, E: *Über die Verwendung von Ionenaustauschern für die Sorption und Trennung von Ketonen.* Acta P 144 (1954), 50 pp, Sw. Kr 8: 00 UDC 661.183.12:66.067.75:547.284

**Nr 2** LEDEN, I and SCHÖÖN, N-H: *The Solubility of Silver Azide and the Formation of Complexes between Silver and Azide Ions.* Acta P 155 (1954), 17 pp, Sw. Kr 4: 00 UDC 662.413.1

**Nr 3** SANDFORD, F, and FRANSSON, S: *The Refractoriness of Some Types of Quartz and Quartzite.* I. Acta P 156 (1954), 27 pp, Sw. Kr 6: 00 UDC 666.346.6:666.361.2

**Nr 4** SÖNNERSKOG, S: *Some Ethers of Cellulose and Starch.* Acta P 157 (1954), 72 pp, Sw. Kr 10: 00 UDC 661.892

**Nr 5** HEDVALL, J A: *Reactions with Activated Solids.* Acta P 163 (1954), 23 pp, Sw. Kr 5: 00 UDC 541.124-188:548.4

**Nr 6** SVENSSON, J: *A New Formula for Particle Size Distribution of Products Produced by Comminution.* Acta P 167 (1955), 53 pp, Sw. Kr 6: 00 UDC 539.215:621.926

**Nr 7** HEDVALL, J A, NORDENGREN, S und LILJEGREN, B: *Über die Thermische Zersetzung von Kalziumsulfat bei Niedrigen Temperaturen.* Acta P 170 (1955), 18 pp Sw. Kr 5: 00 UDC 661.842.532:66.092.4

**Nr 8** DAHLGREN, S-E: *On the Break-down of Thixotropic Materials.* Acta P 171 (1955), 18 pp, Sw. Kr 3: 50 UDC 541.182.025

**Nr 9** SANDFORD, F, and FRANSSON, S: *The Refractoriness of Some Types of Quartz and Quartzite.* II. Acta P 173 (1955), 24 pp, Sw. Kr 5: 00 UDC 666.76:549.514.51

**Nr 10** BJÖRKMAN, L, BJÖRKMAN, M, BRESKY, A, ENEBO, L, and RENNERFELT, J: *Experiments on the Culture of Chlorella for Food Purposes.* Acta P 176 (1955), 18 pp, Sw. Kr 4: 00 UDC 663.11:582.2

**Nr 11** WRANGLÉN, G: *Dendrites and Growth Layers in the Electrocrystallization of Metals.* Acta P 182 (1955), 42 pp, Sw. Kr 6: 50 UDC 669.017:548.232.4:669.017:548.52

**Nr 12** MATTSSON, E: *The Electrode Process in Metal Deposition from Aqueous Solutions.* Acta P 184 (1955), 56 pp, Sw. Kr 6: 50 UDC 541.135:621.357

**Nr 13** EDHBORG, A: *Studies on a Water-Soluble Material from the Masonite Process.* Acta P 197 (1956), 87 pp, Sw. Kr 12: 50 UDC 547.454:542.938:542.941
out of print

# ACTA POLYTECHNICA SCANDINAVICA

## *Chemistry including Metallurgy Series*

**Ch 1** JART, A: *Fat Rancidity. Summaries of Papers Presented at the 2nd Scandinavian Symposium on Fat Rancidity.* (Acta P 242/1958) 72 pp, Sw. Kr 7: 00 UDE 665.112.2

**Ch 2** ERÄMETSÄ, O: *Ion Characteristics; a New Way of Assessing the Chemical Properties of Ions.* (Acta P 249/1958) 22 pp, Sw. Kr 7: 00 UDE 541.7

Price Sw. Kr. 7.00